Article

Cell Reports

# The Protein Tyrosine Phosphatase Receptor Delta Regulates Developmental Neurogenesis

## Graphical Abstract

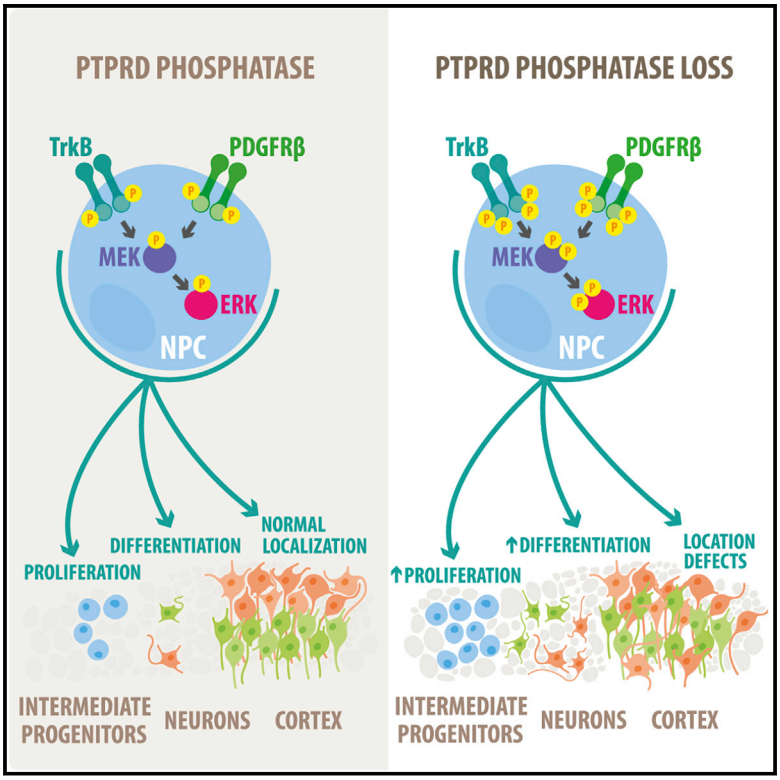


## Highlights

- PTPRD knockdown or knockout induces aberrant increased neurogenesis
- PTPRD null mice have more intermediate progenitors and cortical neurons
- PTPRD regulates neurogenesis by modulating RTK-MEK-ERK pathway activity
- Decreasing MEK/ERK activity or TrkB rescues the perturbations in neurogenesis

## Authors

Hideaki Tomita, Francisca Cornejo, Begoña Aranda-Pino, ..., David R. Kaplan, Freda D. Miller, Gonzalo I. Cancino

## Correspondence

gonzalo.cancino@umayor.cl

## In Brief

Tomita et al. describe how PTPRD, a protein tyrosine phosphatase receptor associated with neurodevelopmental disorders, regulates murine embryonic neurogenesis via the RTK-MEK-ERK signaling pathway. PTPRD null embryos have more intermediate progenitors and, consequently, more cortical neurons, suggesting a mechanism for why loss of PTPRD function results in cognitive dysfunction.

Tomita et al., 2020, Cell Reports *30*, 215–228
January 7, 2020 
https://doi.org/10.1016/j.celrep.2019.11.033

CellPress

Cell Reports
Article



# The Protein Tyrosine Phosphatase Receptor Delta Regulates Developmental Neurogenesis

Hideaki Tomita,[1,8] Francisca Cornejo,[2,8] Begoña Aranda-Pino,[2] Cameron L. Woodard,[1] Constanza C. Rioseco,[1] Benjamin G. Neel,[3] Alejandra R. Alvarez,[4] David R. Kaplan,[1,5,6] Freda D. Miller,[1,5,6,7] and Gonzalo I. Cancino[1,2,9,*]
[1]Program in Neurosciences and Mental Health, Hospital for Sick Children, Toronto M5G 1X8, ON, Canada
[2]Center for Integrative Biology, Facultad de Ciencias, Universidad Mayor, Santiago 8580745, Chile
[3]Laura and Isaac Perlmutter Cancer Center, New York University Langone Health, New York, NY 10016, USA
[4]Departamento de Biología Celular y Molecular, Facultad de Ciencias Biológicas, Pontificia Universidad Católica de Chile, Santiago 8331010, Chile
[5]Institute of Medical Science, University of Toronto, Toronto M5S 1A8, ON, Canada
[6]Department of Molecular Genetics, University of Toronto, Toronto M5S 1A8, ON, Canada
[7]Department of Physiology, University of Toronto, Toronto M5S 1A8, ON, Canada
[8]These authors contributed equally
[9]Lead Contact
*Correspondence: gonzalo.cancino@umayor.cl
https://doi.org/10.1016/j.celrep.2019.11.033

## SUMMARY

**PTPRD is a receptor protein tyrosine phosphatase that is genetically associated with neurodevelopmental disorders. Here, we asked whether *Ptprd* mutations cause aberrant neural development by perturbing neurogenesis in the murine cortex. We show that loss of *Ptprd* causes increases in neurogenic transit-amplifying intermediate progenitor cells and cortical neurons and perturbations in neuronal localization. These effects are intrinsic to neural precursor cells since acute *Ptprd* knockdown causes similar perturbations. PTPRD mediates these effects by dephosphorylating receptor tyrosine kinases, including TrkB and PDGFRβ, and loss of *Ptprd* causes the hyperactivation of TrkB and PDGFRβ and their downstream MEK-ERK signaling pathway in neural precursor cells. Moreover, inhibition of aberrant TrkB or MEK activation rescues the increased neurogenesis caused by knockdown or homozygous loss of *Ptprd*. These results suggest that PTPRD regulates receptor tyrosine kinases to ensure appropriate numbers of intermediate progenitor cells and neurons, suggesting a mechanism for its genetic association with neurodevelopmental disorders.**

## INTRODUCTION

Tyrosine kinase-mediated signaling pathways play a key role in regulating the fate of neural stem cells. Genetic alterations in genes encoding components of these pathways are associated with abnormal development of the human CNS and have been implicated in human neurodevelopmental disorders (Ferguson, 2003; Schubbert et al., 2007; Levitt and Campbell, 2009; Samuels et al., 2009). It has been proposed that mutations that cause these types of conditions may do so, at least in part, by perturbing the development of embryonic neural stem/precursor cells (NPCs) (Ernst, 2016). Alterations in the expression of genes associated with the RAS signaling pathway downstream of receptor tyrosine kinases (RTKs) in NPCs induce aberrant neural development (Bentires-Alj et al., 2006; Ménard et al., 2002; Barnabé-Heider and Miller, 2003; Paquin et al., 2009; Wang et al., 2010; Tsui et al., 2014). Furthermore, the altered expression of genes associated with neurodevelopmental disorders in NPCs also induces abnormal brain development (Mao et al., 2009; Singh et al., 2010; Gallagher et al., 2015; Ernst, 2016), supporting the idea that perturbing the fine balance between maintenance and differentiation of NPCs can have long-lasting consequences for brain function.

Receptor protein tyrosine phosphatase delta (PTPRD), a member of the LAR (leukocyte common antigen-related receptor) family and a regulator of tyrosine kinase signaling, has been associated with several neural disorders (Choucair et al., 2015; Uhl and Martinez, 2019). However, its function and contribution to neural development and the pathogenesis of neural disorders has not yet been studied. These LAR family protein tyrosine phosphatases (PTPs), which also include PTPRS (receptor tyrosine phosphatase sigma) and LAR, are ~60%–70% homologous and are characterized by high levels of expression in the nervous system and a common structure, consisting of extracellular domains with multiple immunoglobulin and fibronectin type III domains and two cytoplasmic phosphatase (PTP) domains (Johnson and Van Vactor, 2003; Chagnon et al., 2004; Östman et al., 2006; Stebbing et al., 2014). Although PTPRD is highly expressed in brain tissue, it has not been associated with neural precursor biology or cortical development. Nevertheless, PTPRD may regulate brain development since (1) *Ptprd* has been genetically associated with several neural disorders, including autism spectrum disorders (ASDs) (Pinto et al., 2010; Levy et al., 2011; Gai et al., 2012; Liu et al., 2016), attention-deficit/hyperactivity disorder (ADHD) (Elia et al., 2010), schizophrenia (Li et al., 2018), obsessive-compulsive disorder (OCD) (Gazzellone et al., 2016), and restless leg syndrome (Schormair et al., 2008; Yang

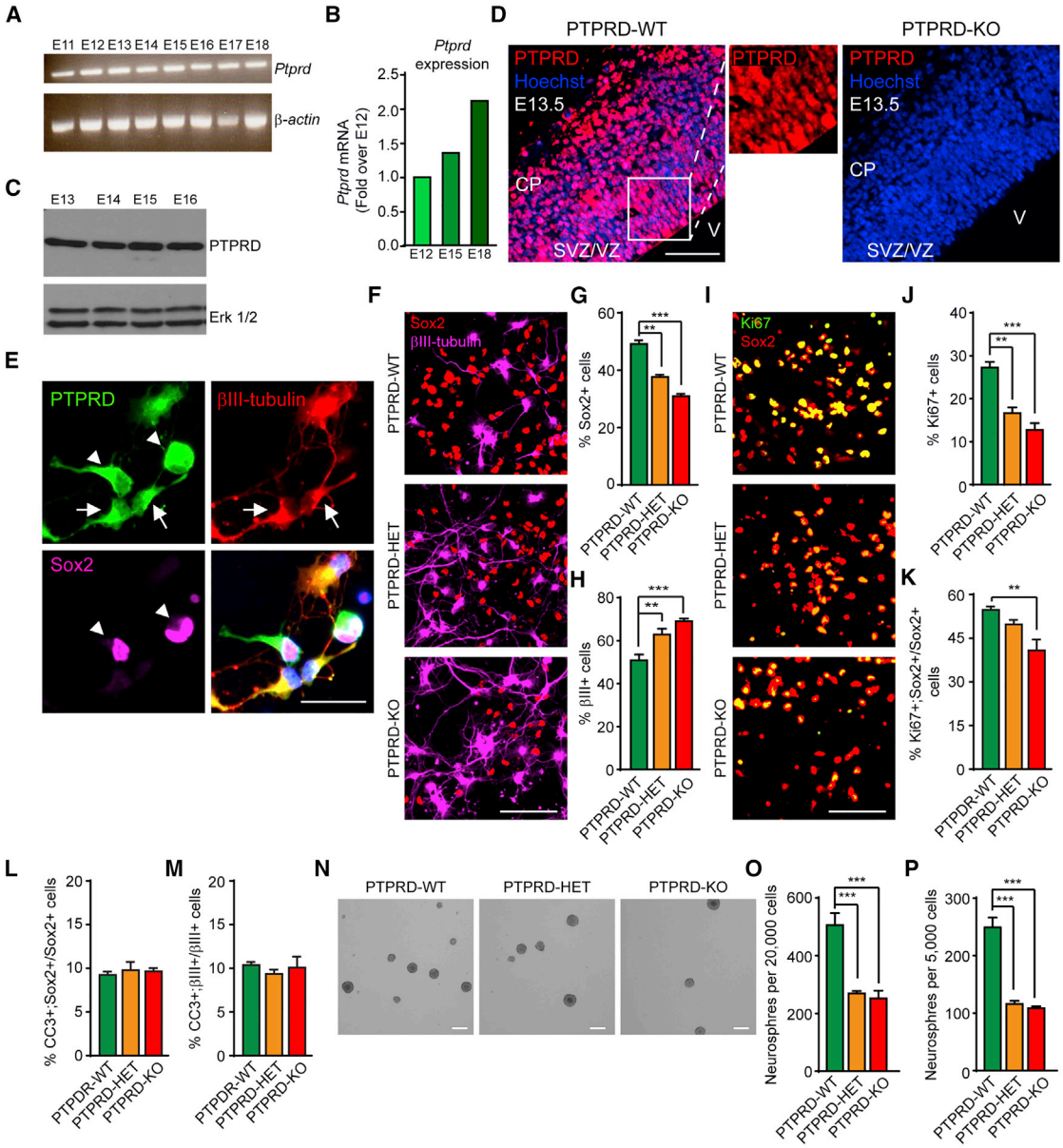


**Figure 1. *Ptprd*$^{+/-}$ and *Ptprd*$^{-/-}$ Mice Show Deficits in Proliferation and Enhancement of Differentiation of Cultured Cortical NPCs**

(A) RT-PCR for *Ptprd* mRNA in the E11–E18 cortex. β-Actin mRNA was used as a loading control.

(B) qRT-PCR for *Ptprd* mRNA in the E12–E18 cortex. Data are expressed as fold over E12 cortex.

(C) Western blot of PTPRD in total cortical lysates from E13 to E16. The blot was reprobed for ERK1/2 as a loading control.

(D) Image of E13.5 *Ptprd*$^{+/+}$ (PTPRD-WT [wild type], left panel) and *Ptprd*$^{-/-}$ (PTPRD-KO [knockout], right panel) cortical sections immunostained for PTPRD (red). The cortical plate (CP), subventricular zone (SVZ), ventricular zone (VZ), and ventricle (V) are denoted. The tissue was counterstained with Hoechst (blue) to show nuclei. The inset shows the magnified image of the boxed area. Scale bar, 200 μm.

(E) Images of E12.5 cortical NPCs cultured for 3 days and then immunostained for PTPRD (green), βIII-tubulin (red), and Sox2 (magenta). Arrows and arrowheads indicate PTPRD$^{+}$ neurons and cortical NPCs, respectively. Scale bar, 50 μm.

(F–M) E12.5 cortical NPCs from single PTPRD-WT, *Ptprd*$^{+/-}$ (PTPRD-HET [heterozygous]), or PTPRD-KO embryos were cultured and analyzed 3 days later.

(F–H) Cells were immunostained for Sox2 (red) and βIII-tubulin (magenta) after 3 days (F) and the proportions of Sox2$^{+}$ (G) or βIII-tubulin$^{+}$ (H) cells were determined. Scale bar, 50 μm. $^{**}p < 0.01$, $^{***}p < 0.001$; n = 3 embryos per genotype.

(I–K) Cells were immunostained for Ki67 (green) and Sox2 (red) after 3 days (I), and the proportion of total Ki67$^{+}$ cells was determined (J). Alternatively, the proportion of total Ki67$^{+}$;Sox2$^{+/+}$ cells over the total Sox2$^{+}$ cells was determined (K).

(L and M) Cells immunostained for cleaved caspase-3 and Sox2 or βIII-tubulin (not shown) after 3 days and the CC3$^{+}$ cells proportion over total Sox2$^{+}$ cells (L) and total βIII-tubulin$^{+}$ (M) was determined. Scale bar, 50 μm. $^{**}p < 0.01$, $^{***}p < 0.001$; n = 3 embryos per genotype.

*(legend continued on next page)*

et al., 2011); (2) studies of *Ptprd*$^{-/-}$ mice suggest a role in motor development (Uetani et al., 2000); (3) *Ptprd* is expressed in the precursor zones of the developing brain (Sommer et al., 1997; Schaapveld et al., 1998; Shishikura et al., 2016); and (4) mutations in *Ptprd* have been reported in neural cancers that likely derive from dysregulated neural precursors (Veeriah et al., 2009; Meehan et al., 2012). Also, PTPRD has been implicated in various cellular processes, including cell growth, proliferation, and migration, as well as axonal growth, pathfinding, and synaptogenesis (Sun et al., 2000; Uetani et al., 2006; Kwon et al., 2010; Takahashi et al., 2012; Yamagata et al., 2015).

How does PTPRD mediate these functions? Notably, the chicken ortholog of PTPRD functions both as a PTP and a homophilic cell adhesion molecule (Wang and Bixby, 1999). However, the major PTPRD isoform expressed in the developing nervous system lacks many of the fibronectin repeats necessary for the adhesion function, suggesting that it regulates neural development via its catalytic activity (Wang and Bixby, 1999; Yang et al., 2005; Zhu et al., 2015; Shishikura et al., 2016). In support of the idea that PTPRD may regulate RTKs involved in brain development, members of the LAR family reportedly dephosphorylate and inactivate RTKs such as Trks and platelet-derived growth factor receptor (PDGFR) (Kulas et al., 1996; Tisi et al., 2000; Yang et al., 2006). Notably, TrkB is necessary for appropriate neurogenesis in the embryonic cortex (Bartkowska et al., 2007). Moreover, in PC12 cells, Trks are substrates of the LAR family (Kypta et al., 1996; Tisi et al., 2000; Xie et al., 2006). PDGFRβ, another substrate of the LAR family (Kulas et al., 1996; Zheng et al., 2011), also regulates the differentiation of NPCs and mouse embryonic fibroblasts (MEFs) (Wu et al., 2008; Hewitt et al., 2012; Funa and Sasahara, 2014). These findings support the idea that the RTKs may be important PTPRD targets within the context of embryonic corticogenesis.

Here, we have investigated the function of PTPRD in the developing brain. Our studies reveal that PTPRD, via its protein tyrosine phosphatase activity, regulates TrkB and PDGFRβ activity, and in so doing, controls developmental cortical neurogenesis. We found that homozygous deletion or knockdown of *Ptprd* increases both the relative proportion of proliferating intermediate progenitor cells and the numbers of cortical neurons. We show that PTPRD interacts with TrkB and PDGFRβ and regulates their activity, and that decreased or absent PTPRD expression leads to increased activation of these receptors and their downstream effectors MEK and ERK. This hyperactivation of RTKs is likely causally related to the increased numbers of intermediate progenitors and neurons, since TrkB or MEK inhibition rescues the increased neurogenesis caused by deletion or knockdown of *Ptprd* in cortical NPCs in culture. We conclude that PTPRD regulates cortical development by preventing the hyper-activation of TrkB and PDGFRβ and their downstream MEK/ERK pathway, thereby regulating the proportion of neurogenic transit-amplifying intermediate progenitor cells and, ultimately, the number of cortical neurons.

## RESULTS

### *Ptprd* Is Expressed in Embryonic Cortical NPCs during Development

Tyrosine kinase-mediated signaling plays a key role in regulating the maintenance and differentiation of neural stem cells. We therefore asked whether PTPRD, which dephosphorylates RTKs, is important in cortical NPCs, focusing on developing murine cortical NPCs during the period of embryonic neurogenesis. We analyzed the expression of *Ptprd* mRNA throughout cortical embryogenesis. RT-PCR analysis (Figure 1A) demonstrated that *Ptprd* was expressed as early as embryonic day 11 (E11), when the cortex is largely composed of NPCs, until E19, when it contains predominantly newborn neurons. Also, data obtained by qRT-PCR suggested that *Ptprd* mRNA may be upregulated from E12 to E18 (Figure 1B). Western blot analysis (Figure 1C) confirmed that PTPRD protein was also present in the embryonic cortex.

To determine which cortical cell types express PTPRD, we immunostained cortical sections at E13.5, when neurogenesis is actively ongoing. This analysis showed that PTPRD was expressed broadly throughout the embryonic cortex and was detectable in cells within the neural precursor regions of the cortex, the ventricular zone (VZ) and subventricular zone (SVZ), and in newly born neurons in the cortical plate (Figure 1D). We confirmed the specificity of this antibody by analyzing similar cortical sections from *Ptprd*$^{-/-}$ mice (Uetani et al., 2000; Figure 1D). To establish conclusively that PTPRD is expressed in cortical NPCs and in newborn neurons, we analyzed E12.5 cortical NPC cultures, which are composed of proliferating radial glial precursors that generate intermediate progenitors and neurons in culture (Gauthier et al., 2007; Yuzwa et al., 2017). Triple labeling for PTPRD, the precursor marker Sox2, and the neuronal marker βIII-tubulin revealed robust PTPRD expression in Sox2$^{+}$ cortical NPCs and βIII-tubulin$^{+}$ neurons (Figure 1E), consistent with our *in vivo* analysis.

### Loss of One or Both Alleles of *Ptprd* Perturbs Cortical NPCs and Enhances Neurogenesis in Culture

To ask whether *Ptprd* is important for cortical NPCs and whether haploinsufficiency, as seen in humans, is sufficient to perturb NPC development, we intercrossed *Ptprd*$^{+/-}$ mice, and then cultured E12.5 cortical NPCs from individual *Ptprd*$^{+/+}$, *Ptprd*$^{+/-}$, or *Ptprd*$^{-/-}$ embryos. Cultures were immunostained for Sox2 and βIII-tubulin 3 days post-plating (Figure 1F). Notably, the loss of either one or both *Ptprd* alleles caused a decrease in the proportion of Sox2$^{+}$ NPCs (Figure 1G). Coincidentally, the proportion of βIII-tubulin$^{+}$ newborn neurons increased (Figure 1H). Thus, the loss of only one *Ptprd* allele is sufficient to perturb cortical NPC biology.

Alterations in the ratio of NPCs to neurons could reflect an increased genesis of neurons and/or a decreased proliferation of cortical NPCs. We therefore quantified NPC proliferation by

(N–P) E13.5 cortical NPCs from single PTPRD-WT, PTPRD-HET, or PTPRD-KO embryos were cultured as primary neurospheres (N) and quantified 6 days later (O). Scale bar, 200 μm. Equal numbers of primary neurosphere cells were then passaged, and the number of secondary neurospheres was quantified 6 days later (P). ***$p < 0.001$; n = 4 embryos per genotype.
Error bars indicate SEMs.

immunostaining for Ki67 (Figure 1I). As seen with total Sox2$^+$ precursor numbers, the proportion of Ki67$^+$ cells was significantly decreased in *Ptprd*$^{+/-}$ and *Ptprd*$^{-/-}$ cultures (Figure 1J). Moreover, the proliferative index, as measured by the ratio of Ki67$^+$, Sox2$^+$ cells over the total Sox2$^+$ population, also decreased significantly in the *Ptprd*$^{-/-}$ cultures (Figure 1K). The decrease in Ki67$^+$, Sox2$^+$ cells did not reflect altered cell death because the proportion of Sox2$^+$ cells expressing cleaved caspase-3 was similar for each genotype (Figure 1L). Similarly, there was no increase in cleaved caspase-3$^+$, βIII$^+$ neurons in these cultures (Figure 1M).

These data indicate that the loss of PTPRD perturbs both NPCs and neurogenesis in cortical cultures. We therefore asked whether it also altered cortical NPC self-renewal in culture using neurosphere assays, which measure the ability of sphere-forming precursor cells to self-renew and generate a new sphere. We cultured E13.5 cortical cells from mice of different genotypes in the presence of fibroblast growth factor 2 (FGF2) and epidermal growth factor (EGF). Six days later, we counted the number of spheres that had formed. Less than half as many neurospheres were generated from *Ptprd*$^{+/-}$ or *Ptprd*$^{-/-}$ cortices relative to their wild-type counterparts, which is consistent with the decreased proportion of Sox2$^+$ precursors in the adherent cultures (Figures 1N and 1O). We then triturated and passaged these neurospheres at equal cell densities and found that when only one *Ptprd* allele was present, there was an ~2.5-fold decrease in the number of secondary spheres formed, and that there was no further decrease with the loss of both *Ptprd* alleles (Figure 1P). Thus, the loss of only one *Ptprd* allele is sufficient to cause deficits in cortical NPC biology in culture.

## *Ptprd* Regulates Cortical NPC Biology in a Cell-Intrinsic Fashion

The observed perturbations in *Ptprd*$^{+/-}$ and *Ptprd*$^{-/-}$ NPCs could be due to an acute requirement for *Ptprd* or to an aberrant developmental history. To distinguish between these two possibilities, we performed knockdown experiments. We tested a small hairpin RNA (shRNA) predicted to be specific for murine *Ptprd* by co-transfecting this shRNA, along with a murine *Ptprd* expression plasmid, into HEK293 cells, and then performing western blots or qRT-PCR. These analyses (Figures 2A and 2B) demonstrated that *Ptprd* shRNA, but not a control shRNA, depleted murine *Ptprd* expression. We then asked whether this shRNA could deplete endogenous *Ptprd* by co-transfecting it with a plasmid encoding nuclear EGFP into cultured E12.5 cortical NPCs. Immunostaining for EGFP and PTPRD 3 days later demonstrated that the *Ptprd* shRNA, but not a control shRNA, knocked down endogenous murine *Ptprd* (Figure 2C).

Having established the efficacy of this shRNA, we asked whether acute *Ptprd* deficiency affected cortical NPCs. *Ptprd* shRNA and the nuclear EGFP expression construct were co-transfected into E12.5 cortical NPC cultures, and 3 days later, the cultures were immunostained for EGFP and either Ki67 or βIII-tubulin (Figures 2D and 2F). *Ptprd* knockdown reduced the proportion of Ki67$^+$ precursors by >2-fold (Figure 2E) and significantly increased the proportion of newborn neurons (Figure 2G), whereas the control hairpin had no effect. The decrease in Ki67$^+$ cells did not reflect altered cell death, because the proportion of EGFP$^+$ cells expressing cleaved caspase-3 were similar in both the control- and *Ptprd* shRNA-transfected cells (Figure S1).

To assess the specificity of these shRNA-dependent effects, we asked whether the knockdown phenotype could be rescued by coincidentally expressing a human PTPRD cDNA construct resistant to the murine *Ptprd* shRNA. We confirmed that the human construct was resistant by co-transfecting it along with the murine *Ptprd* shRNA construct into HEK293 cells and performing a western blot analysis 3 days later (Figure 2H). Initially, we used the human *Ptprd* construct to ask whether the overexpression of PTPRD on its own regulated cortical NPCs by co-transfecting it with the nuclear EGFP construct into E12.5 cortical NPCs. Immunostaining 3 days later showed that PTPRD overexpression significantly increased the proportion of proliferating EGFP$^+$, Ki67$^+$ precursors (Figures 2I and 2J). Moreover, the proportion of EGFP$^+$, βIII-tubulin$^+$ neurons was significantly decreased (Figures 2K and 2L). Thus, PTPRD overexpression is sufficient to increase the proportion of proliferating cortical NPCs.

We next performed shRNA rescue experiments. Cultured NPCs were co-transfected with EGFP and the *Ptprd* shRNA with or without the human PTPRD expression construct. Quantification of EGFP$^+$, Ki67$^+$ cells 3 days later showed that, as expected, *Ptprd* knockdown significantly reduced proliferating NPCs, while the concomitant expression of human PTPRD restored proliferation to levels similar to those seen when PTPRD was overexpressed alone (Figure 2M). Similarly, coincident expression of human PTPRD rescued the increase in neurogenesis observed following shRNA-mediated *Ptprd* knockdown (Figure 2N). Thus, PTPRD acts in a cell-intrinsic fashion to regulate cortical NPC biology, at least in culture.

## Alterations in Radial Glial Precursors, Intermediate Progenitors, and Newborn Neurons in *Ptprd*$^{-/-}$ and *Ptprd*$^{+/-}$ Embryonic Cortices

We next asked whether *Ptprd* perturbed cortical development *in vivo* as was observed *in vitro*. To achieve this, we intercrossed *Ptprd*$^{+/-}$ mice and injected pregnant dams with BrdU at gestational day 13.5 to label proliferating precursors. One hour later mice were sacrificed and the embryos dissected. We then immunostained coronal cortical sections from embryos of different genotypes for bromodeoxyuridine (BrdU) and the radial glial precursor marker Pax6 or the intermediate progenitor marker Tbr2 (Figures 3A and 3C). We also immunostained adjacent sections for Tbr1, which marks early-born cortical neurons, to identify the location of the cortical plate (Figure 3E). This analysis demonstrated that at this short time point, in controls, ~25% of the Pax6$^+$ radial glial precursors were also BrdU$^+$, while ~17% of the Tbr2$^+$ intermediate progenitors were BrdU$^+$. Notably, when *Ptprd* was deficient, the proportion of BrdU$^+$ intermediate progenitors was significantly increased (Figure 3D), while the proportion of BrdU$^+$ radial precursors was unaltered (Figure 3B).

Since intermediate progenitors are the neurogenic transit-amplifying cells in this system, an increase in their relative proliferation may ultimately cause an increase in neuron numbers. To test this idea, we performed similar experiments, but analyzed cortices 24 or 48 h post-BrdU by immunostaining for BrdU and Pax6, Tbr2, or Tbr1 (Figures 3F, 3H, 3J, and S2). This analysis

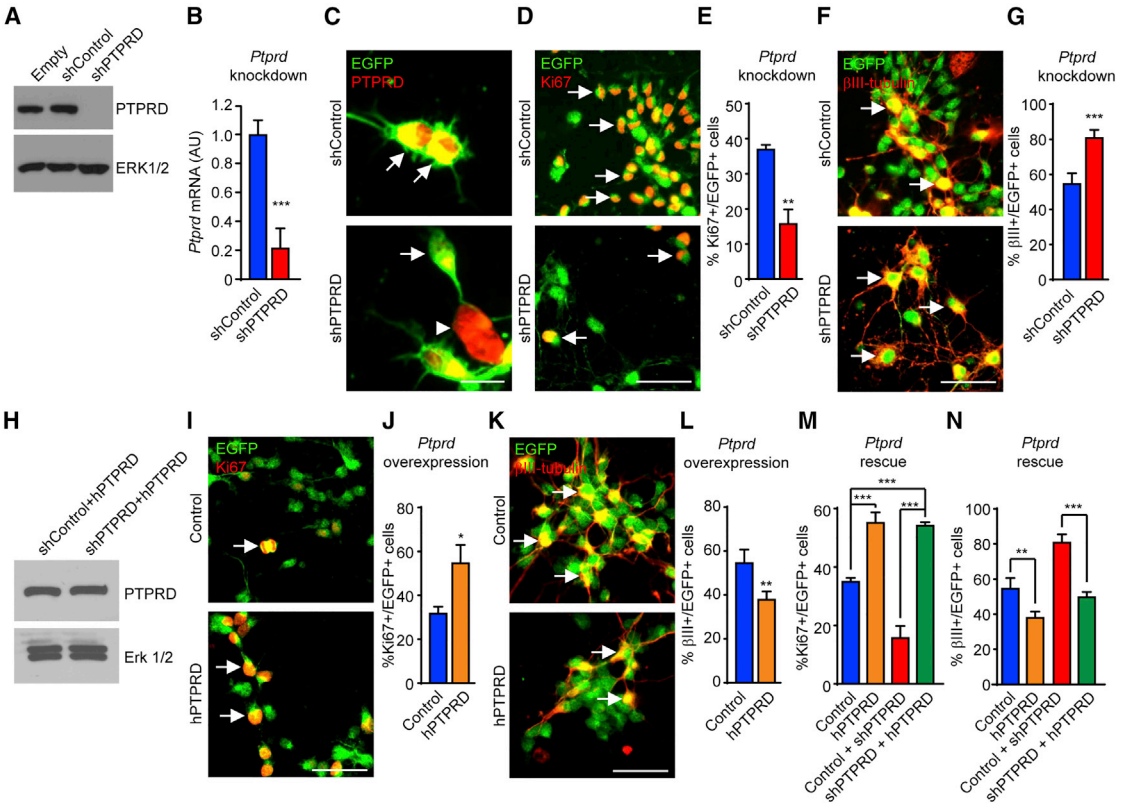


**Figure 2. *Ptprd* Knockdown Decreases Proliferation and Increases Differentiation, While *PTPRD* Overexpression Increases Proliferation and Decreases Differentiation of Cultured Embryonic Cortical NPCs**

(A) Western blot for PTPRD in lysates of HEK293 cells transfected with a murine *Ptprd* expression vector together with control or *Ptprd* shRNAs or with an empty shRNA vector. The blot was reprobed for ERK1/2.

(B) qRT-PCR for *Ptprd* mRNA in HEK293 cells transfected with a murine Ptprd expression vector together with control or *Ptprd* shRNA. ***$p < 0.001$. Data are representative of three independent experiments.

(C) Cortical NPCs with decreased PTPRD expression due to knockdown. E12.5 cortical NPCs were co-transfected with cytoplasmic EGFP and control or *Ptprd* shRNA and then immunostained for EGFP and PTPRD (transfected cells are indicated with arrows and non-transfected cells with arrowheads).

(D–G) E12.5 cortical NPCs were co-transfected with nuclear EGFP and control or *Ptprd* shRNA and then analyzed 3 days later.

(D and E) Cultures were immunostained for EGFP (green, D) and Ki67 (red, D; double-labeled cells are indicated with arrows) and the proportion of total $EGFP^+$ cells that were also positive for Ki67 was quantified (E). **$p < 0.01$. Data are representative of three independent experiments.

(F and G) Cultures were immunostained for EGFP (green, F) and βIII-tubulin (red, F; double-labeled cells are indicated with arrows) and the proportion of total $EGFP^+$ cells that were also positive for βIII-tubulin was quantified (G). ***$p < 0.001$. Data are representative of three independent experiments.

(H–L) E12.5 cortical NPCs were co-transfected with nuclear EGFP and a control or human *Ptprd* expression vector and were analyzed 3 days later. Western blot for PTPRD in lysates of HEK293 cells transfected with a human *Ptprd* expression vector together with control or *Ptprd* shRNAs or with an empty shRNA vector. The blot was reprobed for ERK1/2 (H). Cultures were immunostained for EGFP (green, I) and Ki67 (red, I; double-labeled cells are indicated with arrows), and the proportion of total $EGFP^+$ cells that were also positive for Ki67 was quantified (J). *$p < 0.05$. Data are representative of three independent experiments. Cultures were immunostained for EGFP (green, K) and βIII-tubulin (red, K; double-labeled cells are indicated with arrows) and the proportion of total $EGFP^+$ cells that were also positive for βIII-tubulin was quantified (L). **$p < 0.01$. Data are representative of three independent experiments.

(M and N) E12.5 cortical NPCs cells were co-transfected with nuclear EGFP and control or *Ptprd* shRNA plus or minus an expression construct encoding human *PTPRD*. Cultures were immunostained 3 days later, and the proportions of $EGFP^+$ cells that were also positive for Ki67 (M) or βIII-tubulin (N) were determined. **$p < 0.01$; ***$p < 0.001$. Data are representative of three independent experiments.

Scale bars in all of the panels, 50 μm. In all cases, the error bars denote SEMs.

showed that the loss of one or both alleles of *Ptprd* caused a significant decrease in the proportion of $Pax6^+$ radial precursors that were $BrdU^+$ (Figures 3G, S2A, and S2B). At the same time, there was a significant increase in the proportions of $BrdU^+$ $Tbr2\text{-}^+$ intermediate progenitors and $Tbr1^+$ neurons (Figures 3I, 3K, and S2C–S2F). Thus, PTPRD loss leads to an increase in the genesis of intermediate progenitors and newborn cortical neurons *in vivo*.

To confirm these findings, we also measured the total relative number of radial glial precursors, intermediate progenitors, and $Tbr1^+$ neurons over the same time frame. Specifically, we immunostained cortical sections from *Ptprd* wild-type, heterozygous, and knockout mice at E13.5, E14.5, and E15.5 for Pax6, Tbr2, and Tbr1 (Figures 3L–3N), and quantified total immunopositive cells in a cortical column from the ventricle to the meninges (see Figure S3A). This analysis demonstrated that at E13.5, the

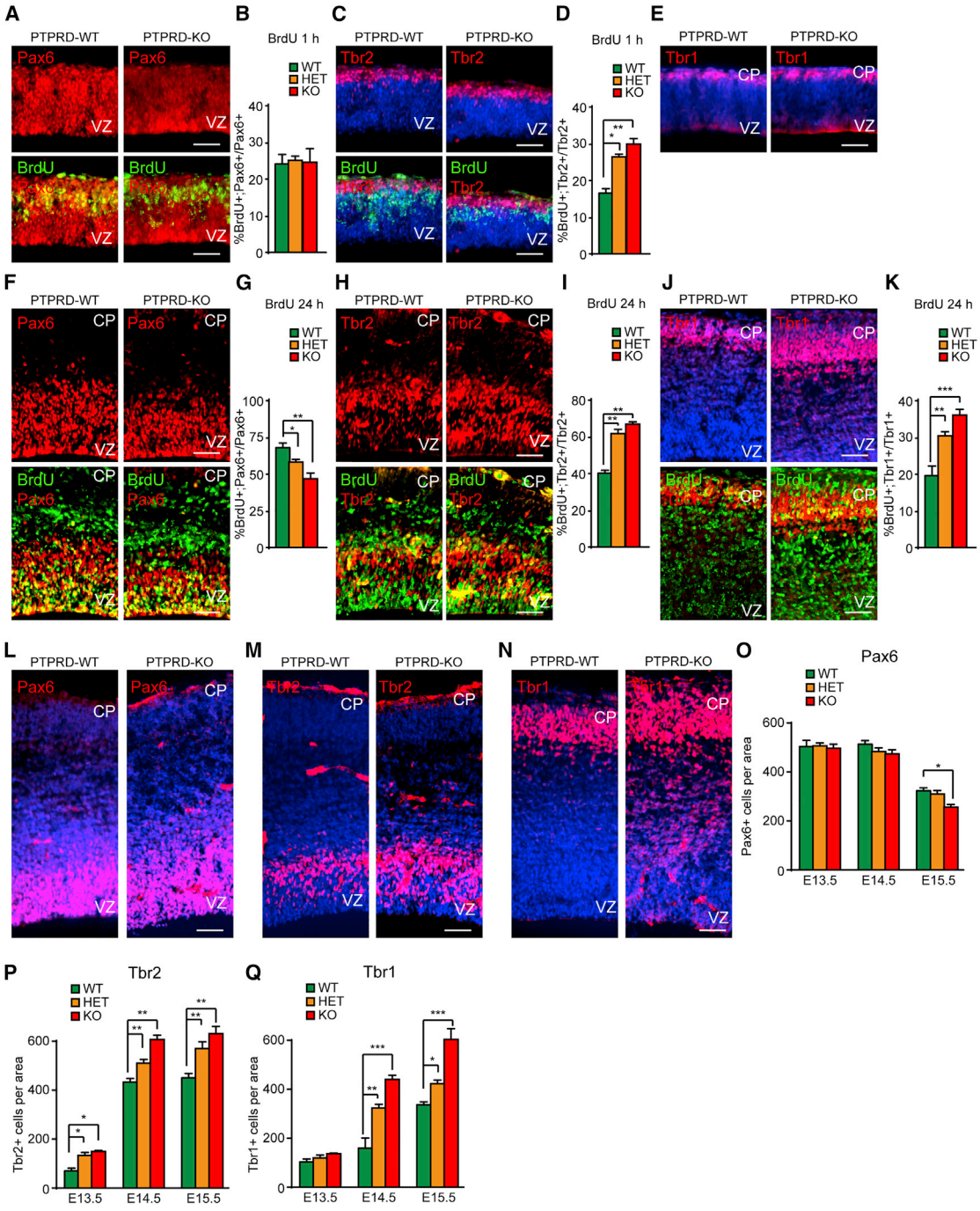


**Figure 3. PTPRD-HET and PTPRD-KO Embryos Display Deficits in Cortical Precursor Proliferation, Neuronal Numbers, and Neuronal Localization**

(A–N) Pregnant mothers were injected with BrdU at E13.5 and 1 (A–E), 24 (F–K), or 48 h later (L–Q; see Figure S2), cortices were removed from their E13.5, E14.5, or E15.5 PTPRD-WT, PTPRD-HET (not shown), and PTPRD-KO progeny, respectively. Coronal cortical sections were then immunostained for BrdU (green; A, C, F, H, and J; see Figure S2), the radial precursor marker Pax6 (red; A, F, and L), the intermediate progenitor marker Tbr2 (red; C, H, and M), or the deep cortical layer marker Tbr1 (red; E, J, and N). These sections were then quantified for the proportion of $BrdU^+$ cells that were also positive for Pax6 (B and G), Tbr2 (D and I), or Tbr1 (K).

(O–Q). Cortical sections as in (A) –(N) were immunostained, and a cortical column of defined width spanning the lateral ventricles to the meninges (see Figure S2) was quantified for the total numbers of cells expressing Pax6 (O), Tbr2 (P), or Tbr1 (Q). *$p < 0.05$; **$p < 0.01$; ***$p < 0.001$; $n = 3$ embryos per genotype. The CP and VZ are denoted.

In all of the images, scale bars represent 50 μm. In all of the panels, the error bars denote SEMs.

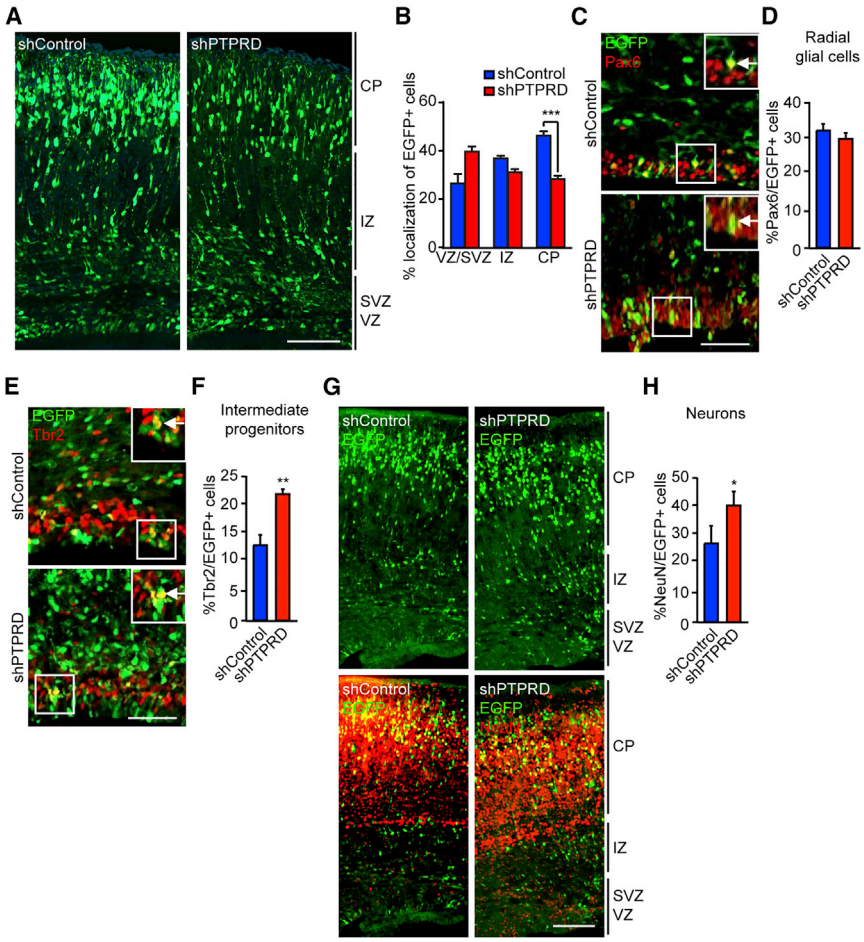


**Figure 4. Acute *Ptprd* Knockdown Increases Intermediate Progenitors and Neurons *In Vivo***

(A–H) E13/E14 cortices were electroporated with EGFP and control or *Ptprd* shRNA, and coronal cortical sections were immunostained 3 days later for EGFP (green) and Pax6 (red; C), Tbr2 (red; E), or NeuN (red; G) and quantified for the relative location of EGFP$^+$ cells in the different cortical regions (B) or for the proportions of EGFP$^+$ cells expressing Pax6 (D), Tbr2 (F), or NeuN (H). The image showed in (A) was generated by stitching. *$p < 0.05$; **$p < 0.01$; ***$p < 0.001$.

In all cases, data are representative of three independent experiments. The boxed regions in (C) and (E) are shown at higher magnification as insets, with arrows indicating double-positive cells. The CP, VZ, SVZ, and intermediate zone (IZ) are indicated.

Scale bar, 50 μm. In all of the panels, the error bars denote SEMs.

only significant change was a modest increase in Tbr2$^+$ intermediate progenitors. However, by E14.5 and E15.5, the numbers of intermediate progenitors and Tbr1$^+$ cortical neurons were both significantly increased with the loss of one or two *Ptprd* alleles (Figures 3P and 3Q). Notably, there was also mislocalization of Tbr1$^+$ cortical neurons; in wild-type mice, neurons were almost all located in the cortical plate, while in the knockout mice, Tbr1$^+$ cells were also scattered throughout the intermediate zone (IZ) (Figure 3N), potentially indicating there was aberrant neuronal migration. By contrast to these alterations in intermediate progenitors and neurons, Pax6$^+$ radial glial precursor numbers were unaltered at E14.5 and were modestly decreased in the *Ptprd* knockouts at E15.5 (Figure 3O). Thus, the loss of one or both *Ptprd* alleles caused an increased genesis of cortical neurons, likely due to a coincident increase in the numbers of intermediate progenitor cells.

## *Ptprd* Is Acutely Required in NPCs during the Period of Cortical Neurogenesis

This aberrant cortical development could be due to a cell-autonomous deficit of *Ptprd* in cortical precursors as seen in culture or, since these are global *Ptprd* knockout mice, it could be due to deficits in cells occurring before the onset of neurogenesis. To distinguish between these possibilities, we used *Ptprd* shRNA to acutely knock down its expression specifically in radial glial cells *in vivo* by electroporating E13/E14 cortices. An EGFP expression construct was co-transfected to mark expressing cells. Immunostaining for EGFP 3 days later demonstrated that the location of electroporated cells was significantly altered by *Ptprd* knockdown, with significantly fewer cells in the cortical plate (Figures 4A and 4B). This altered cellular localization could be due to alterations in the ratios of different types of cells and/or to perturbed migration of cortical neurons, as seen in the knockouts (Figure 3N). To investigate these possibilities, we immunostained electroporated sections for EGFP and for Pax6 (Figure 4C), Tbr2 (Figure 4E), or NeuN (Figure 4G). As seen with global haploinsufficiency or knockout, acute knockdown of *Ptprd* caused a significant increase in the proportion of Tbr2$^+$ intermediate progenitors (Figure 4F) without significantly affecting Pax6$^+$ radial glial precursors (Figure 4D). Coincident with the increase in Tbr2$^+$ intermediate progenitors, the proportion of NeuN$^+$ cells was also significantly increased (Figure 4H). These data indicate that *Ptprd* is acutely required in cortical NPCs and their newborn neuronal progeny and suggest that it may be important for neuronal migration and for regulating the relative proportions of intermediate progenitor cells and newborn neurons.

## The Number and Location of Satb2$^+$ and Tbr1$^+$ Neurons in Embryonic and Postnatal Brain Cortex Are Deregulated in *Ptprd* Null Mice

To ask whether the loss of Ptprd selectively affected Tbr1$^+$ deep-layer neurons or whether it also deregulated later-born cortical neurons, we analyzed the E18.5 cortex, immunostaining for Tbr1 and the superficial layer cortical neuron marker Satb2 (Figures 5A, 5D, and S3B). Quantification of Tbr1$^+$ neurons in the embryonic cortex identified a significant increase in the number of

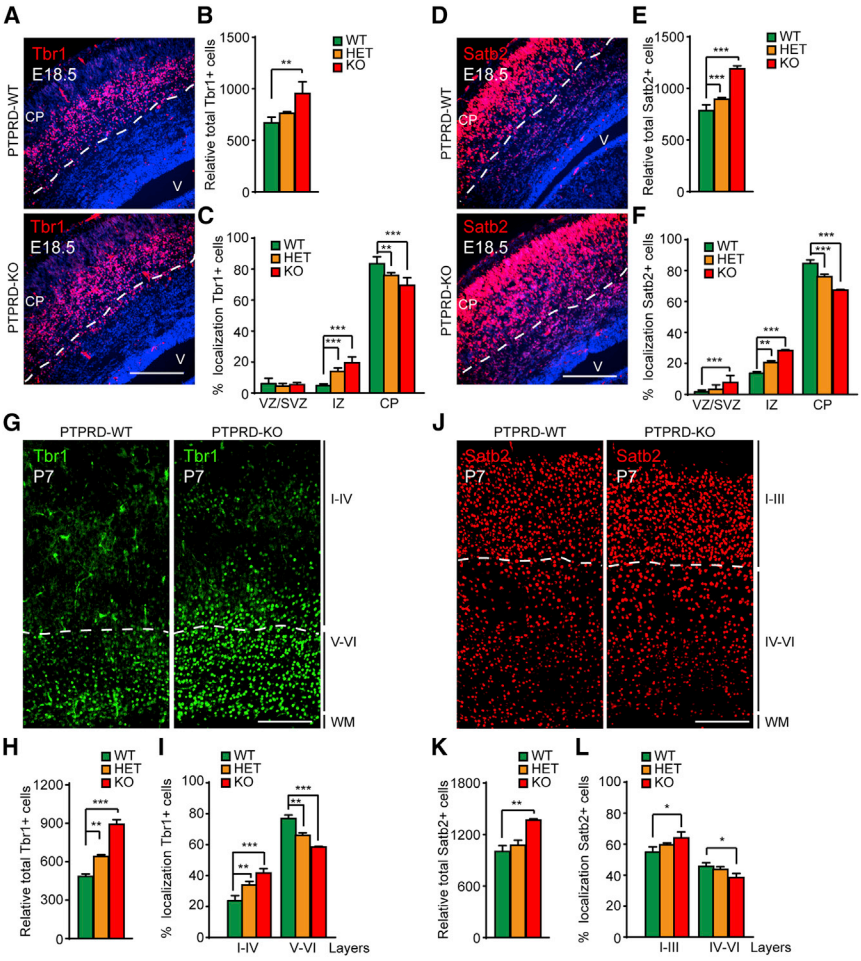


**Figure 5. PTPRD-HET and PTPRD-KO Mice Show Increased Neuronal Number and Mislocalized Neurons**

(A–F) E18.5 PTPRD-WT, PTPRD-HET (not shown), and PTPRD-KO coronal cortical sections were immunostained for Tbr1 (A; red) and Satb2 (D; red; sections were counterstained with Hoechst 33258 in blue) and quantified for relative total number of Tbr1$^+$ cells (B), and for the relative number of Satb2$^+$ cells (E). Also, the relative location of Tbr1$^+$ cells (C) and the location of Satb2$^+$ cells (F) was measured in the different cortical regions. **p < 0.01; ***p < 0.001; n = 3 embryos per genotype. The CP, VZ, SVZ, IZ, and V are denoted.

(G–L) Cortical sections from P7 PTPRD-WT, PTPRD-HET (not shown), and PTPRD-KO mice were immunostained for Tbr1 (G; green) and Satb2 (J; red; sections were counterstained with Hoechst 33258 in blue), and the relative total number of Tbr1$^+$ cells (H) and the relative number of Satb2$^+$ cells (K) were analyzed in the somatosensory cortex. The relative location of Tbr1$^+$ cells (I) and the location of Satb2$^+$ cells (L) were measured in the different cortical layers, which were divided from layer I to IV and from V to VI for Tbr1, and from layer I to III and from IV to VI for Satb2. WM = white matter. *p < 0.05; **p < 0.01; ***p < 0.001; n = 3 mice per genotype.

Scale bar for (A) and (D), 200 μm and (G) and (J), 100 μm. In all of the panels, the error bars denote SEMs.

Tbr1$^+$ cells in the knockout cortices (Figures 5A and 5B), as we had seen at the earlier time points. Notably, we also observed alterations in neuronal location in *Ptprd*$^{+/-}$ and *Ptprd*$^{-/-}$ cortices, with a higher relative proportion of total Tbr1$^+$ neurons in the IZ and a lower proportion in the cortical plate relative to *Ptprd*$^{+/+}$ cortices (Figure 5C). We observed a similar phenotype for Satb2$^+$ neurons. The total number of Satb2$^+$ cells was significantly increased in both the heterozygous and knockout cortices (Figures 5D and 5E), and significantly more of these neurons were in the VZ and IZ, and significantly fewer in the cortical plate (Figure 5F).

These data indicate that the loss of *Ptprd* increases the number of cortical neurons and perturbs their location during embryogenesis. To ask whether these alterations were sustained into postnatal life, we analyzed the number and localization of Tbr1$^+$ and Satb2$^+$ neurons in the somatosensory cortex at postnatal day 7 (P7; Figure S3C). Immunostaining of coronal P7 sections for Tbr1 (Figure 5G) showed that, as we had seen at E18.5, there were significantly more Tbr1$^+$ neurons in *Ptprd*$^{+/-}$ and *Ptprd*$^{-/-}$ cortices (Figure 5H). Moreover, there was a significantly increased proportion of total Tbr1$^+$ cells that were in layers I–IV and a significantly decreased proportion in layers V–VI (Figure 5I). We performed a similar analysis of superficial layer cortical neurons by immunostaining for Satb2 (Figure 5J). In *Ptprd*$^{-/-}$ cortices, we observed significantly more total Satb2$^+$ neurons (Figure 5K), and of these, a significantly higher proportion were in layers I–III and a significantly lower proportion were in layers IV–VI (Figure 5L). Thus, loss of the *Ptprd* gene leads to increased numbers and aberrant positioning of postnatal Satb2$^+$ and Tbr1$^+$ cortical neurons.

## PTPRD Regulates Cortical Neurogenesis by Dephosphorylating Cortical RTKs and Their Downstream MEK-ERK1/2 Signaling Pathway

PTPRD has previously been reported to mediate its effects via phosphatase-dependent and -independent mechanisms. To ask whether the phosphatase domain was important for its effects on cortical NPCs, we generated a human PTPRD construct lacking its PTP domain, but otherwise maintaining its extracellular and transmembrane domains intact (*PTPRDΔCD*; Figure 6A). We confirmed that this construct was expressed. We achieved this by transfecting it into HEK293 cells and performing western blot analysis 3 days later (Figure 6B). We then co-transfected cortical NPCs with an EGFP expression plasmid and the *PTPRDΔCD* construct, with or without control or murine PTPRD shRNA constructs. Three days later, immunostaining for EGFP and Ki67 or βIII-tubulin showed that the ectopic expression of *PTPRDΔCD* alone had no effect on numbers of EGFP$^+$, Ki67$^+$ precursors or EGFP$^+$, βIII-tubulin$^+$ neurons (Figures 6C and 6D), in contrast to the effects of the ectopic expression of

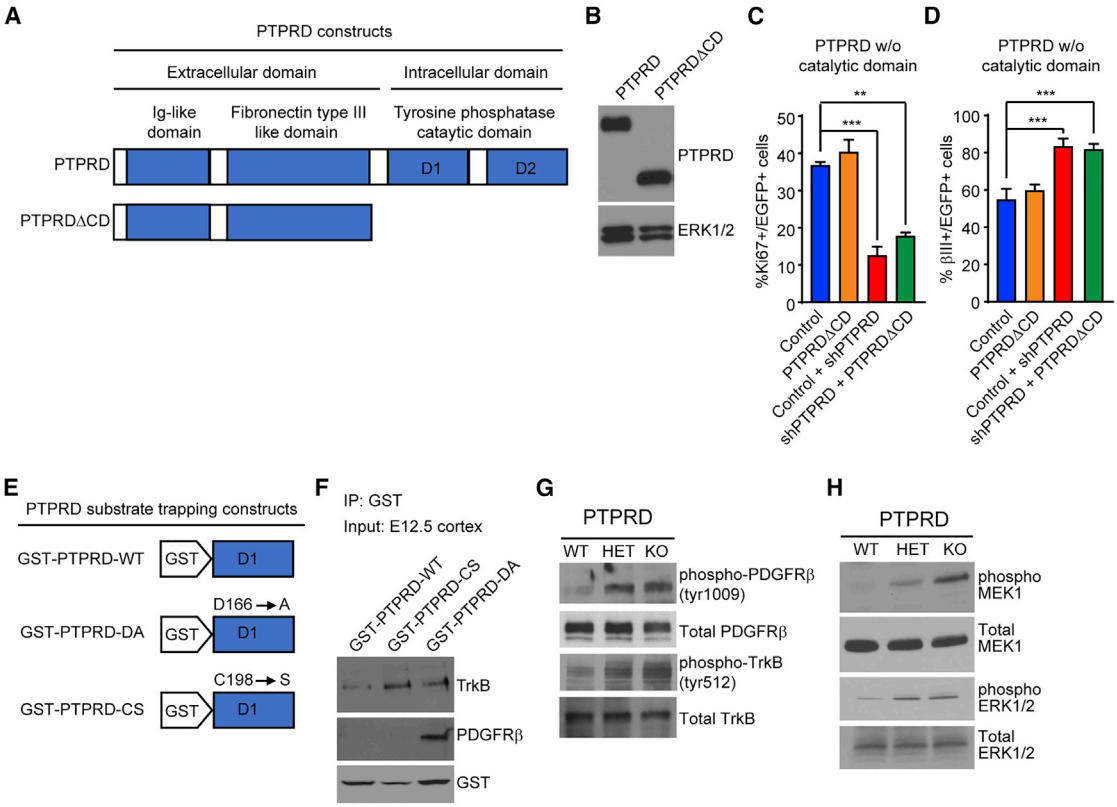


**Figure 6. PTPRD Knockdown Increases the Activity of the Neurogenic RTKs PDGFR and TrkB and Its Downstream Substrate Erk1/2**

(A) Schematic representation of PTPRD protein structure and mutant PTPRD without catalytic domain (PTPRDΔCD) constructs.

(B–D) E12.5 cortical precursor cells were co-transfected with nuclear EGFP and control or *Ptprd* shRNA plus or minus an expression construct encoding PTPRDΔCD. The expression of the construct was detected by western blots using an antibody against PTPRD (B). Cultures were immunostained 3 days later, and the proportion of $EGFP^+$ cells that were also positive for Ki67 (C) or βIII-tubulin (D) was determined. $^{**}p < 0.01$; $^{***}p < 0.001$. Data are representative of three independent experiments.

(E) Schematic representation of PTPRD substrate-trapping constructs; GST-tagged PTPRD (GST-PTPRD-WT) or PTPRD mutated to generate a substrate-trapping protein (GST-PTPRD-CS or GST-PTPRD-DA).

(F) E12.5 cortical lysates were incubated with GST-PTPRD-WT or PTPRD mutated GST-PTPRD-CS or GST-PTPRD-DA. The GST-tagged PTPRD and associated proteins were then pulled down, and the complexes were analyzed by western blots, probed with anti-PDGFRβ, anti-TrkB, or, as a control, anti-GST.

(G and H) Neurospheres were generated from the cortex of E14 PTPRD-WT, PTPRD-HET, and PTPRD-KO mice and analyzed by western blot, probing with antibodies against phospho-PDGFRβ (tyrosine 1,009), phospho-TrkB (Tyr 512), phospho-MEK, or phospho-ERK. Blots were then reprobed with antibodies for the detection of total PDGFRβ, total TrkB, total MEK, or total ERK as loading controls.

full-length human PTPRD (Figures 2I–2N). Furthermore, human PTPRDΔCD was unable to rescue the deficits in proliferating NPCs or newborn neurons caused by shRNA-mediated knockdown of *Ptprd* (Figures 6C and 6D), again, in contrast to the full-length human PTPRD (Figures 2I–2N). Therefore, PTPRD requires its phosphatase activity to regulate cortical development.

PTPRD is thought to act in part by dephosphorylating RTKs. As TrkB and PDGFRβ are known to be important for regulating cortical neurogenesis, we asked whether they may be PTPRD targets in the embryonic cortex. We generated and expressed two different glutathione S-transferase (GST)-tagged "substrate-trapping" mutants of PTPRD (CS, where we replaced C198 to S, and DA, where we replaced D166 to A in the first catalytic domain; Figure 6E) that are predicted to be catalytically inactive but retain the ability to bind substrates (Flint et al., 1997). We then mixed lysates from E12/E13 cortices with either the GST-tagged wild-type PTPRD or the mutant constructs GST-PTPRD-DA or GST-PTPRD-CS and performed GST pull-downs. Western blot analysis showed that TrkB was recovered in pull-downs with both PTPRD substrate-trapping mutants (Figure 6F). PDGFRβ was pulled down with the DA substrate trap mutant (Figure 6F), but not with the CS mutant, potentially because CS mutants of some PTPs are less efficient at trapping substrates (Flint et al., 1997). Probing the same lysates with GST showed that similar amounts of the GST-tagged PTRD protein were recovered in all cases (Figure 6F).

These findings indicate that TrkB and PDGFRβ can interact with PTPRD in the embryonic cortex, supporting the idea that these receptors may be direct PTPRD targets. One prediction of these findings is that if PTPRD levels were reduced, then tyrosine phosphorylation of these receptors would be increased. To test this prediction, we generated and expanded cultures of neurosphere cells from $Ptprd^{+/+}$, $Ptprd^{+/-}$, and $Ptprd^{-/-}$ E13/E14 cortices, and then performed western blots with antibodies

that recognize the phosphorylated, activated forms of TrkB and PDGFRβ. This analysis showed that, relative to total PDGFRβ levels, phosphorylation on tyrosine 1,009, an Src homology 2-containing protein tyrosine phosphatase 2 (SHP-2) and phospholipase Cγ (PLCγ)-association site regulating ERK1/2 activity (Rönnstrand et al., 1999), was increased in cortical neurospheres when either one or both copies of *Ptprd* were mutated (Figure 6G). Similarly, phosphorylation on TrkB tyrosine 512, the SHC association site responsible for regulating Trk-induced ERK1/2 activity (Stephens et al., 1994), was increased in cortical neurospheres in which one or both copies of *Ptprd* were deleted (Figure 6G).

As no exogenous PDGF or neurotrophins were added in these experiments, these results indicate that decreased PTPRD caused increased basal levels of PDGFRβ and TrkB phosphorylation. In this regard, previous studies have shown that TrkB promotes cortical NPC proliferation and differentiation into neurons, in part via activation of the MEK-ERK pathway (Ménard et al., 2002; Barnabé-Heider and Miller, 2003; Bartkowska et al., 2007). Therefore, we performed similar neurosphere experiments and probed western blots with antibodies for phosphorylated activated MEK1 and ERK1/2 to test whether activation of the MEK-ERK pathway was also increased when PTPRD levels were decreased (Figure 6H). This analysis showed that, relative to total MEK1 and ERK1/2 levels, the phosphorylated forms increased when either one or both *Ptprd* alleles were mutated. Thus, the loss of *Ptprd* can deregulate a RTK-dependent signaling pathway important for cortical NPC biology.

### Decreased PTPRD Induces Cortical Neurogenesis via Enhanced Activation of the MEK-ERK Pathway

These data suggest that decreased levels of PTPRD may enhance cortical neurogenesis by increasing RTK-mediated MEK-ERK pathway activation. To directly test this hypothesis, we inhibited MEK in cultured cortical NPCs using two well-characterized chemical inhibitors of MEK, trametinib and PD98059. We confirmed that these two compounds inhibit MEK activity by plating E12.5 cortical NPCs, and 4 h after plating, adding one of the two MEK inhibitors. We then performed western blots to detect phospho-MEK or phospho-ERK1/2 and reprobed the same blots for total MEK or ERK1/2. This analysis showed that both PD98059 and trametinib efficiently inhibited MEK-ERK1/2 activation (Figure 7A). Having confirmed the efficacy of these two drugs, we cultured *Ptprd*$^{+/+}$, *Ptprd*$^{+/-}$, or *Ptprd*$^{-/-}$ E12.5 cortical NPCs, and then 4 h after plating, we added either PD98059 or trametinib. We immunostained cultures for βIII-tubulin 3 days later to test the effect of the inhibitors on neurogenesis (Figure 7B). This analysis showed that PD98059 significantly inhibited the genesis of βIII$^{+}$ neurons on its own (Figure 7C), as previously published. Moreover, as predicted, loss of either one or both *Ptprd* alleles increased the proportion of newborn neurons. The inhibition of MEK by either PD98059 or trametinib rescued the *Ptprd* knockout-mediated increase in the relative proportion of neurons back to levels seen with the control *Ptprd*$^{+/+}$ (Figure 7C). We confirmed these results by performing knockdown experiments. Specifically, we cultured E12.5 cortical NPCs and co-transfected them with EGFP and either control or *Ptprd* shRNA. Four hours after transfection, we added either PD98059 or trametinib, and 3 days later, we immunostained these cultures for EGFP and βIII-tubulin. Quantification showed that the inhibition of MEK by either PD98059 or trametinib rescued the *Ptprd* knockdown-mediated increase in the relative proportion of neurons back down to levels seen with the control shRNA (Figures 7D and 7E).

Pharmacological inhibitors may have off-target effects. We therefore performed rescue experiments by genetically knocking down either TrkB or MEK. Initially, we tested shRNAs predicted to be specific for *Trkb* or *Mek* (Jensen et al., 2016) by transfecting them independently into HEK293 cells and performing western blots. These analyses demonstrated that *Trkb* shRNA (Figure 7F) or *Mek* shRNA (Figure 7H) but not a control shRNA decreased TrkB or MEK protein, respectively. We then co-transfected cultured cortical precursors with EGFP and the *Ptprd* shRNA plus or minus shRNAs against *Trkb* or *Mek*. Quantification of EGFP$^{+}$, βIII-tubulin$^{+}$ cells 3 days later showed that coincident TrkB knockdown rescued the increased proportion of neurons observed following shRNA-mediated *Ptprd* knockdown (Figure 7G). Similar results were obtained when MEK was knocked down (Figure 7I). Thus, *Ptprd* regulates normal cortical neurogenesis by maintaining appropriate levels of phosphorylated and activated RTKs such as PDGFRβ and TrkB, and thus the activity of the downstream MEK-ERK1/2 pathway.

## DISCUSSION

Alterations in neural precursor cell biology are thought to lead to perturbations in cortical development and contribute to the etiology of neurodevelopmental disorders (Ernst, 2016). Here, we analyzed the role of the tyrosine phosphatase PTPRD in NPCs during embryonic cortical development. *Ptprd*, the gene that encodes this protein, is associated with several neurodevelopmental disorders, including obsessive-compulsive disorder, ASDs, and intellectual disability (Choucair et al., 2015; Uhl and Martinez, 2019). We show that *Ptprd* is a key determinant of embryonic neurogenesis, controlling the numbers of neurogenic intermediate progenitor cells and, ultimately, the number of cortical neurons. In cultured E12.5 cortical precursors, we found that heterozygous and homozygous deletion of *Ptprd* induces a relative decrease in proliferating precursors and a concomitant increase in newborn neurons. Similarly, *in vivo* analysis of *Ptprd*$^{+/-}$ and *Ptprd*$^{-/-}$ embryonic cortices showed that the loss of *Ptprd* caused aberrant NPC development, with increased numbers of intermediate progenitors and newborn neurons. The culture phenotypes and the aberrant *in vivo* increase in intermediate progenitors could be mimicked by acute knockdown of *Ptprd*, indicating that there is an ongoing, cell-intrinsic requirement for this gene during the period of cortical neurogenesis. The loss of *Ptprd* also had more long-term effects; at later time points embryonically and during early postnatal development, in *Ptprd*$^{-/-}$ mice there were more cortical neurons and these neurons were aberrantly positioned. Thus, we conclude that PTPRD regulates NPC biology and plays a key role in embryonic cortical development. Disruption of this important role in humans who carry one mutant allele of the *Ptprd* gene may provide a partial explanation for their neurodevelopmental disorders.

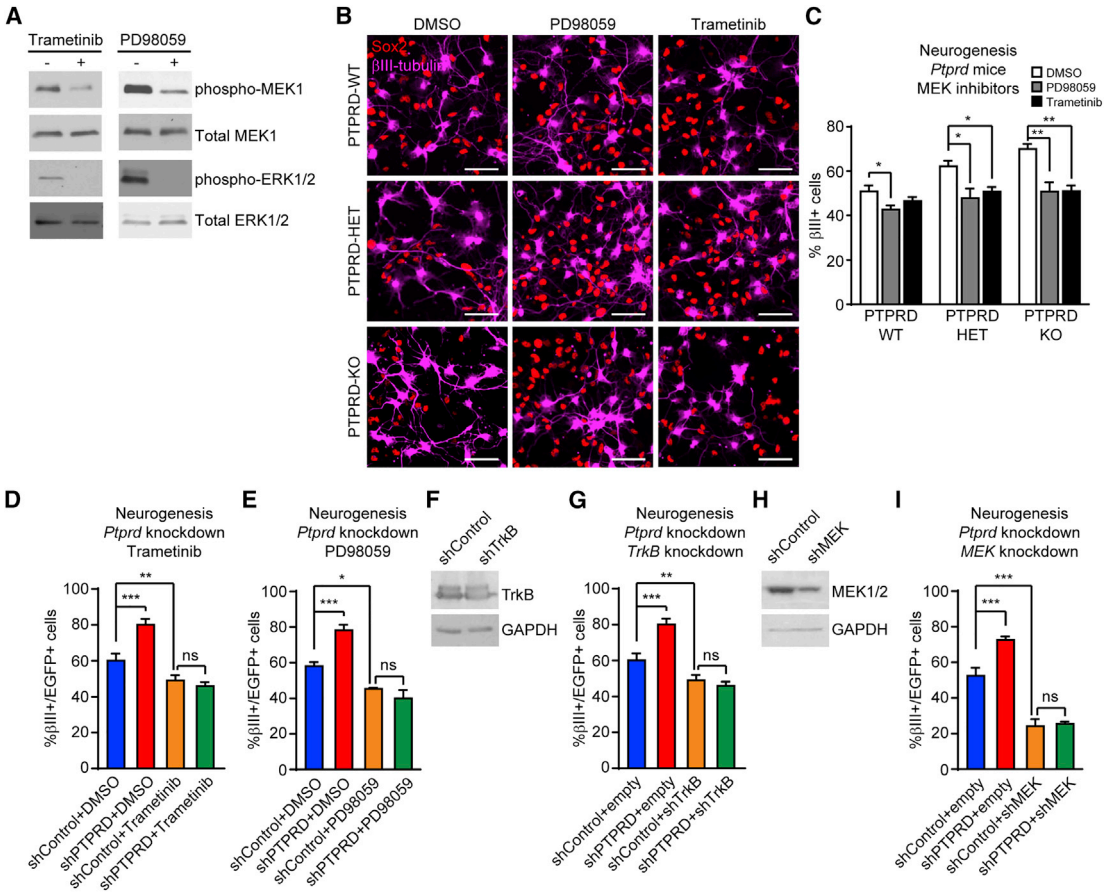


**Figure 7. Decreasing MEK/ERK1/2 Activity or TrkB Rescues the Perturbations in Neurogenesis Induced by *Ptprd* Knockdown**

(A) E12.5 cortical NPC cultures were treated or not treated with MEK/ERK inhibitors, trametinib, or PD98059. Western blot of phospho-MEK and phospho-ERK. Blots were then reprobed with antibodies for total MEK or total ERK as loading controls.

(B and C) E12.5 cortical NPCs from single PTPRD-WT, PTPRD-HET, or PTPRD-KO embryos were treated or not treated with 100 nM trametinib (black column) or 50 μM PD98059 (gray column). Three days later, cultures were immunostained for EGFP and βIII-tubulin (B), and the proportion of transfected newborn neurons was quantified (C). Scale bar, 50 μm. *p < 0.05; **p < 0.01. n = 7 for WT experiments; n = 4 for HET and KO experiments.

(D and E) E12.5 cortical NPCs were co-transfected with nuclear EGFP and control or *Ptprd* shRNA and treated or not treated with 100 nM trametinib (D) or 50 μM PD98059 (E). Three days later, cultures were immunostained for EGFP and βIII-tubulin, and the proportion of transfected newborn neurons was determined. *p < 0.05; **p < 0.01; ***p < 0.001; ns, not significant. Data are representative of three independent experiments.

(F and H) Western blot for TrkB (F) or MEK1/2 (H) in lysates of HEK293 cells transfected with control or *TrkB* shRNA (F) or *MEK* shRNA (H) vector. The blot was reprobed for glyceraldehyde 3-phosphate dehydrogenase (GAPDH).

(G and I) E12.5 cortical NPCs were co-transfected with nuclear EGFP and control or *Ptprd* shRNA and co-transfected with TrkB shRNA (G) or MEK shRNA (I). Three days later, cultures were immunostained for EGFP and βIII-tubulin, and the proportion of transfected newborn neurons was determined. **p < 0.01; ***p < 0.001; ns, not significant. Data are representative of three independent experiments.

Error bars denote SEMs.

How does PTPRD increase the numbers of intermediate progenitors and neurons? At a mechanistic level, one way it could do so is by regulating RTKs associated with proliferation, maintenance, and/or differentiation of cortical precursors since PTPRD is a transmembrane receptor with an intracellular tyrosine phosphatase domain. Here, we show that PTPRD interacts with and regulates the activity of PDGFRβ and TrkB, both of which have been associated with NPC biology (Bartkowska et al., 2007; Xu et al., 2013; Funa and Sasahara, 2014). Specifically, we show that PDGFRβ and TrkB interacted with PTPRD in ''trapping assays,'' and we found increased levels of phosphorylated PDGFRβ and TrkB on tyrosines 1,009 and 512, respectively, in lysates obtained from neurospheres from *Ptprd*$^{+/-}$ and *Ptprd*$^{-/-}$ embryos. These sites regulate the activation of the MEK-ERK1/2 pathway (Stephens et al., 1994; Rönnstrand et al., 1999), and, consistent with this, we found that MEK and ERK1/2 were hyperactivated. Moreover, we found that pharmacologically inhibiting this hyperactivation was sufficient to rescue the increased genesis of neurons that occurred in culture upon acute or long-term loss of *Ptprd*.

These findings support a model in which PTPRD interacts with TrkB, PDGFRβ, and/or potentially other RTKs in cortical precursor cells, where it acts to dephosphorylate these receptors and dampen their activity under basal conditions. When PTPRD is

decreased as it is in mice or humans with the mutation of one *Ptprd* allele, this would lead to hyperactivation of these RTKs and thus aberrantly high activation of the MEK-ERK pathway. We propose that this hyperactivation causes an expansion of the intermediate progenitor pool, either by an increase in their genesis from radial glial precursors and/or by an increase in the number of divisions that they can undergo before they differentiate into neurons. This increase in the numbers of intermediate progenitors would be sufficient to explain the increased number of cortical neurons that we observe in $Ptprd^{+/-}$ and $Ptprd^{-/-}$ mice. Such an increase in the proportion of intermediate progenitors is thought to be responsible, in part, for the increased number of neurons that are generated in the human cortex (Molnár, 2011). Support for this model comes from previous work showing that the hyperactivation of TrkB by the overexpression of brain-derived neurotrophic factor (BDNF) in the embryonic cortical neuroepithelium was sufficient to cause an acute increase in proliferating precursors and an increase in newborn cortical neurons (Bartkowska et al., 2007). While these authors did not distinguish between radial glial precursor cells and intermediate progenitors, this phenotype is very similar to what we report here with acute knockdown of *Ptprd* in embryonic cortical radial glial precursors: a net increase in cortical precursors due to increased intermediate progenitors and a concomitant increase in newborn cortical neurons.

In addition to increased intermediate progenitors and cortical neurons, we observed neuronal mislocalization with global *Ptprd* deletion. This mislocalization was not apparently specific to neuronal subpopulations, since we observed it for both $Tbr1^{+}$ deep-layer neurons and $Satb2^{+}$ upper-layer neurons. This neuronal mislocalization likely explains our observation that in $Ptprd^{+/-}$ and $Ptprd^{-/-}$ cortices, there were decreased numbers of $BrdU^{+}$ cells in the cortical plate in spite of the fact that BrdU-labeled neurons were increased. Similar results were observed following *Ptprd* knockdown by *in utero* electroporation (Figures 4A and 4B). There are multiple potential explanations for this neuronal mislocalization. One explanation is that aberrant RTK activation leads to perturbed morphological development of newborn neurons, and these neurons are thus unable to align with and migrate along radial glial fibers to the cortical plate. In support of this idea, we quantified the neurite number and found that $Ptprd^{-/-}$ neurons have fewer neurites than $Ptprd^{+/+}$ neurons (data not shown), as seen previously by others (Shishikura et al., 2016; Nakamura et al., 2017). A second possibility is that neurons require appropriate environmental cues to recognize when they are in the right location, and perhaps the hyperactivation of RTKs that occurs in the absence of PTPRD "blinds" them to other extrinsic cues that may act through the same downstream signaling pathways. Finally, perhaps the aberrantly increased genesis of newborn cortical neurons is sufficient in and of itself to lead to the misplacement of a certain proportion of these excess neurons.

*Ptprd* has been genetically associated with the neurological disorders ASDs (Pinto et al., 2010; Levy et al., 2011; Gai et al., 2012; Liu et al., 2016), restless leg syndrome (Schormair et al., 2008; Yang et al., 2011), ADHD (Elia et al., 2010), and OCD (Pauls et al., 2014; Gazzellone et al.; 2016), suggesting that it could regulate common cellular networks that are relevant to these neurodevelopmental disorders, and is consistent with the notion that PTPRD is a key regulator of brain development. In most of these neurodevelopmental disorders, *Ptprd* is deleted. Notably, our data show that the loss of one or both *Ptprd* alleles in mice is sufficient to perturb cortical NPC biology, and in so doing to have long-lasting effects on neuronal numbers and localization, thereby providing a potential explanation for at least some of the cognitive alterations seen in humans with *Ptprd* mutations.

## STAR★METHODS

Detailed methods are provided in the online version of this paper and include the following:

- KEY RESOURCES TABLE
- LEAD CONTACT AND MATERIALS AVAILABILITY
- EXPERIMENTAL MODEL AND SUBJECT DETAILS
  - Animals
  - Cortical precursor cell cultures
  - Neurosphere cultures
- METHOD DETAILS
  - Plasmid generation
  - Cortical precursor cell cultures transfection and quantification
  - *In Utero* Electroporation
  - Immunocytochemistry and histological analysis
  - Antibodies concentrations
  - RT-PCR
  - qRT-PCR
  - Western Blotting
  - Substrate trapping
- QUANTIFICATION AND STATISTICAL ANALYSIS
- DATA AND CODE AVAILABILITY

### SUPPLEMENTAL INFORMATION

Supplemental Information can be found online at https://doi.org/10.1016/j.celrep.2019.11.033.

### ACKNOWLEDGMENTS

This work was funded by the National Fund for Scientific and Technological Development (FONDECYT) Regular grant 1161374 to G.I.C., Canadian Institute of Health Research (CIHR) grants MOP-38021 and MOP-14446 to F.D.M. and D.R.K., CARE-Chile-UC grant AFB170005 to A.R.A., and National Cancer Institute (NCI) grant R01CA49152 to B.G.N. G.I.C. was also funded by CONICYT/PCI REDES 180113, Universidad Mayor start-up grant, and an International Brain Research Organization Return Home Fellowship. F.C. holds FONDECYT postdoctorado 3190517 and Universidad Mayor postdoctoral fellowships. We thank Jessica Molina, Sarah Burns, Benigno Aquino, and Felipe Serrano for technical assistance.

### AUTHOR CONTRIBUTIONS

G.I.C. and H.T. conceptualized, designed, performed, and analyzed most of the experiments and co-wrote the paper. F.C. designed, performed, and analyzed some of the experiments and co-wrote the paper. B.A.-P. and C.L.W. performed and analyzed some of the *in vivo* assays. C.C.R. performed and analyzed some of the culture experiments. B.G.N. conceptualized the biochemistry experiments and provided the *Ptprd* mice. A.R.A., D.R.K., and F.D.M. conceptualized and designed experiments, analyzed data, and co-wrote the paper.

## DECLARATION OF INTERESTS

The authors declare no competing interests

Received: February 21, 2018
Revised: October 10, 2019
Accepted: November 7, 2019
Published: January 7, 2020

## REFERENCES

Barnabé-Heider, F., and Miller, F.D. (2003). Endogenously produced neurotrophins regulate survival and differentiation of cortical progenitors via distinct signaling pathways. J. Neurosci. *23*, 5149–5160.

Bartkowska, K., Paquin, A., Gauthier, A.S., Kaplan, D.R., and Miller, F.D. (2007). Trk signaling regulates neural precursor cell proliferation and differentiation during cortical development. Development *134*, 4369–4380.

Bentires-Alj, M., Kontaridis, M.I., and Neel, B.G. (2006). Stops along the RAS pathway in human genetic disease. Nat. Med. *12*, 283–285.

Cancino, G.I., Yiu, A.P., Fatt, M.P., Dugani, C.B., Flores, E.R., Frankland, P.W., Josselyn, S.A., Miller, F.D., and Kaplan, D.R. (2013). p63 Regulates adult neural precursor and newly born neuron survival to control hippocampal-dependent Behavior. J. Neurosci. *33*, 12569–12585.

Cancino, G.I., Fatt, M.P., Miller, F.D., and Kaplan, D.R. (2015). Conditional ablation of p63 indicates that it is essential for embryonic development of the central nervous system. Cell Cycle *14*, 3270–3281.

Carpenter, A.E., Jones, T.R., Lamprecht, M.R., Clarke, C., Kang, I.H., Friman, O., Guertin, D.A., Chang, J.H., Lindquist, R.A., Moffat, J., et al. (2006). CellProfiler: image analysis software for identifying and quantifying cell phenotypes. Genome Biol. *7*, R100.

Chagnon, M.J., Uetani, N., and Tremblay, M.L. (2004). Functional significance of the LAR receptor protein tyrosine phosphatase family in development and diseases. Biochem. Cell Biol. *82*, 664–675.

Choucair, N., Mignon-Ravix, C., Cacciagli, P., Abou Ghoch, J., Fawaz, A., Mégarbané, A., Villard, L., and Chouery, E. (2015). Evidence that homozygous PTPRD gene microdeletion causes trigonocephaly, hearing loss, and intellectual disability. Mol. Cytogenet. *8*, 39.

Elia, J., Gai, X., Xie, H.M., Perin, J.C., Geiger, E., Glessner, J.T., D'arcy, M., deBerardinis, R., Frackelton, E., Kim, C., et al. (2010). Rare structural variants found in attention-deficit hyperactivity disorder are preferentially associated with neurodevelopmental genes. Mol. Psychiatry *15*, 637–646.

Ernst, C. (2016). Proliferation and differentiation deficits are a major convergence point for neurodevelopmental disorders. Trends Neurosci. *39*, 290–299.

Ferguson, S.S. (2003). Receptor tyrosine kinase transactivation: fine-tuning synaptic transmission. Trends Neurosci. *26*, 119–122.

Flint, A.J., Tiganis, T., Barford, D., and Tonks, N.K. (1997). Development of "substrate-trapping" mutants to identify physiological substrates of protein tyrosine phosphatases. Proc. Natl. Acad. Sci. USA *94*, 1680–1685.

Funa, K., and Sasahara, M. (2014). The roles of PDGF in development and during neurogenesis in the normal and diseased nervous system. J. Neuroimmune Pharmacol. *9*, 168–181.

Gai, X., Xie, H.M., Perin, J.C., Takahashi, N., Murphy, K., Wenocur, A.S., D'arcy, M., O'Hara, R.J., Goldmuntz, E., Grice, D.E., et al. (2012). Rare structural variation of synapse and neurotransmission genes in autism. Mol. Psychiatry *17*, 402–411.

Gallagher, D., Voronova, A., Zander, M.A., Cancino, G.I., Bramall, A., Krause, M.P., Abad, C., Tekin, M., Neilsen, P.M., Callen, D.F., et al. (2015). Ankrd11 is a chromatin regulator involved in autism that is essential for neural development. Dev. Cell *32*, 31–42.

Gauthier, A.S., Furstoss, O., Araki, T., Chan, R., Neel, B.G., Kaplan, D.R., and Miller, F.D. (2007). Control of CNS cell-fate decisions by SHP-2 and its dysregulation in Noonan syndrome. Neuron *54*, 245–262.

Gazzellone, M.J., Zarrei, M., Burton, C.L., Walker, S., Uddin, M., Shaheen, S.M., Coste, J., Rajendram, R., Schachter, R.J., Colasanto, M., et al. (2016). Uncovering obsessive-compulsive disorder risk genes in a pediatric cohort by high-resolution analysis of copy number variation. J. Neurodev. Disord. *8*, 36.

Hewitt, K.J., Shamis, Y., Knight, E., Smith, A., Maione, A., Alt-Holland, A., Sheridan, S.D., Haggarty, S.J., and Garlick, J.A. (2012). PDGFRβ expression and function in fibroblasts derived from pluripotent cells is linked to DNA demethylation. J. Cell Sci. *125*, 2276–2287.

Jensen, K.J., Moyer, C.B., and Janes, K.A. (2016). Network architecture predisposes an enzyme to either pharmacologic or genetic targeting. Cell Syst. *2*, 112–121.

Johnson, K.G., and Van Vactor, D. (2003). Receptor protein tyrosine phosphatases in nervous system development. Physiol. Rev. *83*, 1–24.

Kulas, D.T., Goldstein, B.J., and Mooney, R.A. (1996). The transmembrane protein-tyrosine phosphatase LAR modulates signaling by multiple receptor tyrosine kinases. J. Biol. Chem. *271*, 748–754.

Kwon, S.K., Woo, J., Kim, S.Y., Kim, H., and Kim, E. (2010). Trans-synaptic adhesions between netrin-G ligand-3 (NGL-3) and receptor tyrosine phosphatases LAR, protein-tyrosine phosphatase delta (PTPdelta), and PTPsigma via specific domains regulate excitatory synapse formation. J. Biol. Chem. *285*, 13966–13978.

Kypta, R.M., Su, H., and Reichardt, L.F. (1996). Association between a transmembrane protein tyrosine phosphatase and the cadherin-catenin complex. J. Cell Biol. *134*, 1519–1529.

Levitt, P., and Campbell, D.B. (2009). The genetic and neurobiologic compass points toward common signaling dysfunctions in autism spectrum disorders. J. Clin. Invest. *119*, 747–754.

Levy, D., Ronemus, M., Yamrom, B., Lee, Y.H., Leotta, A., Kendall, J., Marks, S., Lakshmi, B., Pai, D., Ye, K., et al. (2011). Rare de novo and transmitted copy-number variation in autistic spectrum disorders. Neuron *70*, 886–897.

Li, J., Yoshikawa, A., Brennan, M.D., Ramsey, T.L., and Meltzer, H.Y. (2018). Genetic predictors of antipsychotic response to lurasidone identified in a genome wide association study and by schizophrenia risk genes. Schizophr. Res. *192*, 194–204.

Liu, X., Shimada, T., Otowa, T., Wu, Y.Y., Kawamura, Y., Tochigi, M., Iwata, Y., Umekage, T., Toyota, T., Maekawa, M., et al. (2016). Genome-wide Association Study of Autism Spectrum Disorder in the East Asian Populations. Autism Res. *9*, 340–349.

Mao, Y., Ge, X., Frank, C.L., Madison, J.M., Koehler, A.N., Doud, M.K., Tassa, C., Berry, E.M., Soda, T., Singh, K.K., et al. (2009). Disrupted in schizophrenia 1 regulates neuronal progenitor proliferation via modulation of GSK3beta/beta-catenin signaling. Cell *136*, 1017–1031.

Meehan, M., Parthasarathi, L., Moran, N., Jefferies, C.A., Foley, N., Lazzari, E., Murphy, D., Ryan, J., Ortiz, B., Fabius, A.W., et al. (2012). Protein tyrosine phosphatase receptor delta acts as a neuroblastoma tumor suppressor by destabilizing the aurora kinase A oncogene. Mol. Cancer *11*, 6.

Ménard, C., Hein, P., Paquin, A., Savelson, A., Yang, X.M., Lederfein, D., Barnabé-Heider, F., Mir, A.A., Sterneck, E., Peterson, A.C., et al. (2002). An essential role for a MEK-C/EBP pathway during growth factor-regulated cortical neurogenesis. Neuron *36*, 597–610.

Molnár, Z. (2011). Evolution of cerebral cortical development. Brain Behav. Evol. *78*, 94–107.

Nakamura, F., Okada, T., Shishikura, M., Uetani, N., Taniguchi, M., Yagi, T., Iwakura, Y., Ohshima, T., Goshima, Y., and Strittmatter, S.M. (2017). Protein Tyrosine Phosphatase δ Mediates the Sema3A-Induced Cortical Basal Dendritic Arborization through the Activation of Fyn Tyrosine Kinase. J. Neurosci. *37*, 7125–7139.

Östman, A., Hellberg, C., and Böhmer, F.D. (2006). Protein-tyrosine phosphatases and cancer. Nat. Rev. Cancer *6*, 307–320.

Paquin, A., Hordo, C., Kaplan, D.R., and Miller, F.D. (2009). Costello syndrome H-Ras alleles regulate cortical development. Dev. Biol. *330*, 440–451.

Pauls, D.L., Abramovitch, A., Rauch, S.L., and Geller, D.A. (2014). Obsessive-compulsive disorder: an integrative genetic and neurobiological perspective. Nat. Rev. Neurosci. *15*, 410–424.

Pinto, D., Pagnamenta, A.T., Klei, L., Anney, R., Merico, D., Regan, R., Conroy, J., Magalhaes, T.R., Correia, C., Abrahams, B.S., et al. (2010). Functional impact of global rare copy number variation in autism spectrum disorders. Nature *466*, 368–372.

Rönnstrand, L., Arvidsson, A.K., Kallin, A., Rorsman, C., Hellman, U., Engström, U., Wernstedt, C., and Heldin, C.H. (1999). SHP-2 binds to Tyr763 and Tyr1009 in the PDGF beta-receptor and mediates PDGF-induced activation of the Ras/MAP kinase pathway and chemotaxis. Oncogene *18*, 3696–3702.

Samuels, I.S., Saitta, S.C., and Landreth, G.E. (2009). MAP'ing CNS development and cognition: an ERKsome process. Neuron *61*, 160–167.

Schaapveld, R.Q., Schepens, J.T., Bächner, D., Attema, J., Wieringa, B., Jap, P.H., and Hendriks, W.J. (1998). Developmental expression of the cell adhesion molecule-like protein tyrosine phosphatases LAR, RPTPdelta and RPTPsigma in the mouse. Mech. Dev. *77*, 59–62.

Schormair, B., Kemlink, D., Roeske, D., Eckstein, G., Xiong, L., Lichtner, P., Ripke, S., Trenkwalder, C., Zimprich, A., Stiasny-Kolster, K., et al. (2008). PTPRD (protein tyrosine phosphatase receptor type delta) is associated with restless legs syndrome. Nat. Genet. *40*, 946–948.

Schubbert, S., Shannon, K., and Bollag, G. (2007). Hyperactive Ras in developmental disorders and cancer. Nat. Rev. Cancer *7*, 295–308.

Shishikura, M., Nakamura, F., Yamashita, N., Uetani, N., Iwakura, Y., and Goshima, Y. (2016). Expression of receptor protein tyrosine phosphatase δ, PTPδ, in mouse central nervous system. Brain Res. *1642*, 244–254.

Singh, K.K., Ge, X., Mao, Y., Drane, L., Meletis, K., Samuels, B.A., and Tsai, L.H. (2010). Dixdc1 is a critical regulator of DISC1 and embryonic cortical development. Neuron *67*, 33–48.

Sommer, L., Rao, M., and Anderson, D.J. (1997). RPTPdelta and the novel protein tyrosine phosphatase RPTP psi are expressed in restricted regions of the developing central nervous system. Dev. Dyn. *208*, 48–61.

Stebbing, J., Lit, L.C., Zhang, H., Darrington, R.S., Melaiu, O., Rudraraju, B., and Giamas, G. (2014). The regulatory roles of phosphatases in cancer. Oncogene *33*, 939–953.

Stephens, R.M., Loeb, D.M., Copeland, T.D., Pawson, T., Greene, L.A., and Kaplan, D.R. (1994). Trk receptors use redundant signal transduction pathways involving SHC and PLC-gamma 1 to mediate NGF responses. Neuron *12*, 691–705.

Sun, Q.L., Wang, J., Bookman, R.J., and Bixby, J.L. (2000). Growth cone steering by receptor tyrosine phosphatase delta defines a distinct class of guidance cue. Mol. Cell. Neurosci. *16*, 686–695.

Takahashi, H., Katayama, K., Sohya, K., Miyamoto, H., Prasad, T., Matsumoto, Y., Ota, M., Yasuda, H., Tsumoto, T., Aruga, J., and Craig, A.M. (2012). Selective control of inhibitory synapse development by Slitrk3-PTPδ trans-synaptic interaction. Nat. Neurosci. *15*, 389–398, S1–S2.

Tisi, M.A., Xie, Y., Yeo, T.T., and Longo, F.M. (2000). Downregulation of LAR tyrosine phosphatase prevents apoptosis and augments NGF-induced neurite outgrowth. J. Neurobiol. *42*, 477–486.

Tsui, D., Voronova, A., Gallagher, D., Kaplan, D.R., Miller, F.D., and Wang, J. (2014). CBP regulates the differentiation of interneurons from ventral forebrain neural precursors during murine development. Dev. Biol. *385*, 230–241.

Uetani, N., Kato, K., Ogura, H., Mizuno, K., Kawano, K., Mikoshiba, K., Yakura, H., Asano, M., and Iwakura, Y. (2000). Impaired learning with enhanced hippocampal long-term potentiation in PTPdelta-deficient mice. EMBO J. *19*, 2775–2785.

Uetani, N., Chagnon, M.J., Kennedy, T.E., Iwakura, Y., and Tremblay, M.L. (2006). Mammalian motoneuron axon targeting requires receptor protein tyrosine phosphatases sigma and delta. J. Neurosci. *26*, 5872–5880.

Uhl, G.R., and Martinez, M.J. (2019). PTPRD: neurobiology, genetics, and initial pharmacology of a pleiotropic contributor to brain phenotypes. Ann. N Y Acad. Sci. *1451*, 112–129.

Veeriah, S., Brennan, C., Meng, S., Singh, B., Fagin, J.A., Solit, D.B., Paty, P.B., Rohle, D., Vivanco, I., Chmielecki, J., et al. (2009). The tyrosine phosphatase PTPRD is a tumor suppressor that is frequently inactivated and mutated in glioblastoma and other human cancers. Proc. Natl. Acad. Sci. USA *106*, 9435–9440.

Wang, J., and Bixby, J.L. (1999). Receptor tyrosine phosphatase-delta is a homophilic, neurite-promoting cell adhesion molecular for CNS neurons. Mol. Cell. Neurosci. *14*, 370–384.

Wang, J., Weaver, I.C., Gauthier-Fisher, A., Wang, H., He, L., Yeomans, J., Wondisford, F., Kaplan, D.R., and Miller, F.D. (2010). CBP histone acetyltransferase activity regulates embryonic neural differentiation in the normal and Rubinstein-Taybi syndrome brain. Dev. Cell *18*, 114–125.

Wu, E., Palmer, N., Tian, Z., Moseman, A.P., Galdzicki, M., Wang, X., Berger, B., Zhang, H., and Kohane, I.S. (2008). Comprehensive dissection of PDGF-PDGFR signaling pathways in PDGFR genetically defined cells. PLoS One *3*, e3794.

Xie, Y., Massa, S.M., Ensslen-Craig, S.E., Major, D.L., Yang, T., Tisi, M.A., Derevyanny, V.D., Runge, W.O., Mehta, B.P., Moore, L.A., et al. (2006). Protein-tyrosine phosphatase (PTP) wedge domain peptides: a novel approach for inhibition of PTP function and augmentation of protein-tyrosine kinase function. J. Biol. Chem. *281*, 16482–16492.

Xu, G., Shen, J., Ishii, Y., Fukuchi, M., Dang, T.C., Zheng, Y., Hamashima, T., Fujimori, T., Tsuda, M., Funa, K., and Sasahara, M. (2013). Functional analysis of platelet-derived growth factor receptor-β in neural stem/progenitor cells. Neuroscience *238*, 195–208.

Yamagata, A., Sato, Y., Goto-Ito, S., Uemura, T., Maeda, A., Shiroshima, T., Yoshida, T., and Fukai, S. (2015). Structure of Slitrk2-PTPδ complex reveals mechanisms for splicing-dependent trans-synaptic adhesion. Sci. Rep. *5*, 9686.

Yang, T., Yin, W., Derevyanny, V.D., Moore, L.A., and Longo, F.M. (2005). Identification of an ectodomain within the LAR protein tyrosine phosphatase receptor that binds homophilically and activates signalling pathways promoting neurite outgrowth. Eur. J. Neurosci. *22*, 2159–2170.

Yang, T., Massa, S.M., and Longo, F.M. (2006). LAR protein tyrosine phosphatase receptor associates with TrkB and modulates neurotrophic signaling pathways. J. Neurobiol. *66*, 1420–1436.

Yang, Q., Li, L., Yang, R., Shen, G.Q., Chen, Q., Foldvary-Schaefer, N., Ondo, W.G., and Wang, Q.K. (2011). Family-based and population-based association studies validate PTPRD as a risk factor for restless legs syndrome. Mov. Disord. *26*, 516–519.

Yang, G., Cancino, G.I., Zahr, S.K., Guskjolen, A., Voronova, A., Gallagher, D., Frankland, P.W., Kaplan, D.R., and Miller, F.D. (2016). A Glo1-Methylglyoxal Pathway that Is Perturbed in Maternal Diabetes Regulates Embryonic and Adult Neural Stem Cell Pools in Murine Offspring. Cell Rep. *17*, 1022–1036.

Yuzwa, S.A., Borrett, M.J., Innes, B.T., Voronova, A., Ketela, T., Kaplan, D.R., Bader, G.D., and Miller, F.D. (2017). Developmental Emergence of Adult Neural Stem Cells as Revealed by Single-Cell Transcriptional Profiling. Cell Rep. *21*, 3970–3986.

Zheng, W., Lennartsson, J., Hendriks, W., Heldin, C.H., and Hellberg, C. (2011). The LAR protein tyrosine phosphatase enables PDGF β-receptor activation through attenuation of the c-Abl kinase activity. Cell. Signal. *23*, 1050–1056.

Zhu, Q., Tan, Z., Zhao, S., Huang, H., Zhao, X., Hu, X., Zhang, Y., Shields, C.B., Uetani, N., and Qiu, M. (2015). Developmental expression and function analysis of protein tyrosine phosphatase receptor type D in oligodendrocyte myelination. Neuroscience *308*, 106–114.

## STAR★METHODS

### KEY RESOURCES TABLE

| REAGENT or RESOURCE | SOURCE | IDENTIFIER |
|---|---|---|
| Antibodies | | |
| Chicken polyclonal GFP | Abcam | Cat#: ab13970; RRID:AB_300798 |
| Mouse monoclonal BrdU (clone Bu20a) | Bio-Rad | Cat#: MCA2483T; RRID:AB_1055584 |
| Rabbit polyclonal PTPRD | Abcam | Cat#: ab103013; RRID:AB_10710803 |
| Rabbit polyclonal Pax6 | Covance | Cat#: 901302; RRID:AB_2749901 |
| Rabbit monoclonal Tbr2 (clone EPR19012) | Abcam | Cat#: ab183991; RRID:AB_2721040 |
| Mouse monoclonal Ki67 (clone B56) | BD Biosciences | Cat#: 550609; RRID:AB_393778 |
| Rabbit polyclonal Tbr1 | Abcam | Cat#: ab31940; RRID:AB_2200219 |
| Mouse monoclonal Satb2 (clone SATBA4B10) | Abcam | Cat#: ab51502; RRID:AB_882455 |
| Mouse monoclonal βIII-tubulin | Covance | Cat#: MMS-435P; RRID:AB_2313773 |
| Rabbit polyclonal βIII-tubulin | Covance | Cat#: PRB-435P; RRID:AB_291637 |
| Rabbit polyclonal cleaved caspase 3 | Millipore | Cat#: AB3623; RRID:AB_91556 |
| Rabbit monoclonal Sox2 (clone D6D9) | Cell signaling | Cat#: 3579; RRID:AB_2195767 |
| Goat polyclonal Sox2 | Santa Cruz Biotech | Cat#: sc-17320; RRID:AB_2286684 |
| Rabbit polyclonal Erk1/2 | Santa Cruz Biotech | Cat#: sc-292838; RRID:AB_2650548 |
| Rabbit monoclonal phospho-Erk1/2 (clone D13.14.4E) | Cell signaling | Cat#: 4370; RRID:AB_2315112 |
| Rabbit monoclonal TrkB (clone 80E3) | Cell signaling | Cat#: 4603; RRID:AB_2155125 |
| Rabbit monoclonal phospho-TrkB (clone C35G9) | Cell signaling | Cat#: 4619; RRID:AB_10235585 |
| Rabbit monoclonal PDGFR (clone D1E1E) | Cell signaling | Cat#: 3174; RRID:AB_2162345 |
| Rabbit monoclonal phospho-PDGFR (clone 23B2) | Cell signaling | Cat#: 2992; RRID:AB_390728 |
| Rabbit monoclonal MEK1/2 (clone 47E6) | Cell signaling | Cat#: 9126; RRID:AB_331778 |
| Rabbit monoclonal phospho-MEK1/2 (clone 166F8) | Cell signaling | Cat#: 2338; RRID:AB_490903 |
| Alexa Fluor 555-conjugated donkey anti-mouse IgG | Invitrogen | Cat#: A-31572; RRID:AB_162543 |
| Alexa Fluor 555-conjugated donkey anti-rabbit IgG | Invitrogen | Cat#: A-31570; RRID:AB_2536180 |
| Alexa Fluor 488-conjugated donkey anti-mouse IgG | Invitrogen | Cat#: R37114; RRID:AB_2556542 |
| Alexa Fluor 488-conjugated donkey anti- rabbit IgG | Invitrogen | Cat#: R37118; RRID:AB_2556546 |
| Alexa Fluor 488-conjugated chicken anti-rat IgG | Invitrogen | Cat#: A-21470; RRID:AB_10561519 |
| Cy3-conjugated donkey anti-goat antibody | Jackson ImmunoResearch | Cat#: 705-165-147; RRID:AB_2307351 |
| HRP-conjugated donkey anti-mouse IgG | Invitrogen | Cat#: A16011; RRID:AB_2534685 |
| HRP-conjugated donkey anti-rabbit IgG | Invitrogen | Cat#: A16023; RRID:AB_2534697 |
| Chemicals, Peptides, and Recombinant Proteins | | |
| HBSS | GIBCO | Cat#: 14170112 |
| Neurobasal medium | GIBCO | Cat#: 21103049 |
| L-glutamine | GIBCO | Cat#: A2916801 |
| B27 supplement | GIBCO | Cat#: 17504044 |
| Penicillin-streptomycin | GIBCO | Cat#: 15140148 |
| FGF2 | Sigma | Cat#: F0291 |
| Laminin | Sigma | Cat#: CC095-M |
| Poly-D-lysine | Sigma Aldrich | Cat#. P4707 |
| Lipofectamine LTX and Plus Reagent | Invitrogen | Cat#: 15338100 |
| Opti-MEM | GIBCO | Cat#: 31985062 |
| PD98059 | Selleck chemicals | Cat#: S1177 |
| Trametinib | Selleck chemicals | Cat#: S2673 |
| EGF | Sigma | Cat#: E9644 |

(*Continued on next page*)

*Continued*

| REAGENT or RESOURCE | SOURCE | IDENTIFIER |
|---|---|---|
| Heparin | Sigma | Cat#: H0200000 |
| Permount | Fisher Scientific | Cat#: SP15 |
| Hoechst 33258 | Sigma | Cat#: 861405 |
| BrdU | Sigma | Cat#: B5002 |
| Tri-Reagent | Sigma | Cat#: 93289 |
| DNase I | Thermo Scientific | Cat#: EN0525 |
| glutathione Sepharose 4b beads | GE Healthcare | Cat#: GE17-0756-01 |
| Critical Commercial Assays | | |
| SuperScript III Reverse Transcriptase kit | Invitrogen | Cat#: 18080044 |
| SuperScript IV Reverse Transcriptase Kit | Invitrogen | Cat#: 18090050 |
| Taqman Fast Advance Mater Mix | Applied Biosystems | Cat#: 4444965 |
| Experimental Models: Organisms/Strains | | |
| B6;129-Ptprd $^{<tm1Yiw>}$ | The RIKEN Bioresource research center | Cat# RBRC04925; RRID:IMSR_RBRC04925 |
| C57BL/6N-A < tm1Brd > Ptprd < tm2a(KOMP)Wtsi > /WtsiOrl | Wellcome Trust Sanger Institute | Cat# EM:11805; RRID:IMSR_EM:11805 |
| CD1 | Charles River Laboratory | Strain Code 022 |
| Oligonucleotides | | |
| PTPRD mice (B6;129-Ptprd $^{<tm1Yiw>}$) genotyping primer sequence, forward: Delta-WT-F: 5′-CCAGCAGAGGCACA GAAACTC-3′ | Uetani et al., 2000 | N/A |
| PTPRD mice (B6;129-Ptprd $^{<tm1Yiw>}$) genotyping primer sequence, reverse: Delta-WT-R: 5′-CTGGAATTGTCTCA CTTCCCTC-3′ | Uetani et al., 2000 | N/A |
| PTPRD mice (B6;129-Ptprd $^{<tm1Yiw>}$) genotyping primer sequence, mutant: Delta-Mut: 5′-GACTGCCTTGGGAAA AGCGCCTCC-3′ | Uetani et al., 2000 | N/A |
| PTPRD mice (C57BL/6N-A < tm1Brd > Ptprd < tm2a(KOMP)Wtsi > /WtsiOrl) genotyping primer sequence, forward: Ptprd_111547_F: 5′- TCACCTCGCTGTTCTTC CTG-3′ | Wellcome Trust Sanger Institute | https://www.infrafrontier.eu/sites/infrafrontier.eu/files/upload/public/pdf/genotype_protocols/EM11805_geno.pdf |
| PTPRD mice (C57BL/6N-A < tm1Brd > Ptprd < tm2a(KOMP)Wtsi > /WtsiOrl) genotyping primer sequence, reverse: Ptprd_111547_R: 5′- CTTCTCAGTGCCCAACC CTC-3′ | Wellcome Trust Sanger Institute | https://www.infrafrontier.eu/sites/infrafrontier.eu/files/upload/public/pdf/genotype_protocols/EM11805_geno.pdf |
| PTPRD mice (C57BL/6N-A < tm1Brd > Ptprd < tm2a(KOMP)Wtsi > /WtsiOrl) genotyping primer sequence, mutant: CAS_R1_Term: 5′- TCGTGGTATCGTTATGC GCC-3′ | Wellcome Trust Sanger Institute | https://www.infrafrontier.eu/sites/infrafrontier.eu/files/upload/public/pdf/genotype_protocols/EM11805_geno.pdf |
| qPCR *Ptprd*-specific primer sequence, forward: PTPRD -F: 5′- CTTCAGTGCTGCTGTCTTGG-3′ | This paper | N/A |
| qPCR *Ptprd*-specific primer sequence, reverse: PTPRD -R: 5′- TCATTTGCAGGAACATCAGG-3′ | This paper | N/A |
| qPCR *β-actin*-specific primer sequence, forward: β-actin-F: 5′-GATGACGATATCGCTGCGCTG-3′ | This paper | N/A |
| qPCR *β-actin*-specific primer sequence, reverse: β-actin-R: 5′- GTACGACCAGAGGCATACAGG-3′ | This paper | N/A |
| murine *Ptprd* shRNA-specific sequence: 5′- GGTTGAAAG CAAATGATAA-3′ | This paper | N/A |
| control shRNA-specific sequence: 5′-TCCCAACTGTCAC GTTCTC-3′ | This paper | N/A |

(*Continued on next page*)

*Continued*

| REAGENT or RESOURCE | SOURCE | IDENTIFIER |
|---|---|---|
| murine shRNA *TrkB*-specific sequence: 5′-GCTCCTTAAG GATAACGAA-3′ | This paper | N/A |
| murine *Mek1/2* shRNA-specific sequence: 5′-GCTGATC CACCTGGAGATCAA-3′ | Kevin Janes Lab | Addgene # 72570 |
| Recombinant DNA | | |
| pCMV-mPTPRD-Myc/DDK | Origene | Cat#: MR227256 |
| pCMV-hPTPRD-Myc/DDK | Origene | Cat#: RC214115 |
| murine PTPRD cDNA ORF clone | Origene | Cat#: MG226685 |
| pEF-DEST51 | Invitrogen | Cat#: 12285011 |
| pSUPER.retro.Neo+GFP | Oligoengine | Cat#: VEC-PRT-0005/0006 |
| pENTR-GST6P-1 | Eric Campeau Lab | Addgene #17741 |
| pLKO.3G | Christophe Benoist & Diane Mathis Lab | Addgene # 14748 |
| pCLX-UBI-VenusN | Patrick Salmon Lab | Addgene # 27247 |
| pCMV6-mMek-Myc-Flag | Origene | Cat#: PS100016 |
| Software and Algorithms | | |
| CellProfiler software | Carpenter et al., 2006 | https://cellprofiler.org/; RRID:SCR_007358 |
| Prism 8 | GraphPad | https://www.graphpad.com/; RRID:SCR_002798 |
| Adobe Illustrator CC | Adobe | https://www.adobe.com/products/illustrator.html; RRID: SCR_010279 |
| Adobe Photoshop CC | Adobe | https://www.adobe.com/products/photoshop.html; RRID: SCR_014199 |
| ZEN software | Zeiss | https://www.zeiss.com/microscopy/int/products/microscope-software/zen.html; RRID: SCR_013672 |
| LAS X software | Leica | https://www.leica-microsystems.com/products/microscope-software/p/leica-las-x-ls/; RRID: SCR_013673 |

## LEAD CONTACT AND MATERIALS AVAILABILITY

Further information and requests for resources and reagents should be directed to and will be fulfilled by the Lead Contact. Also, plasmids generated in this study have not been deposited for public access yet but are available without restriction from the Lead Contact, Dr. Gonzalo I. Cancino (gonzalo.cancino@umayor.cl).

## EXPERIMENTAL MODEL AND SUBJECT DETAILS

### Animals

Animal use was approved by the Hospital for Sick Children Animal Care Committee in accordance with the Canadian Council of Animal Care policies and Universidad Mayor Animal Care Committee. Two different strains of *Ptprd* mice were used in this work and were maintained as heterozygous. The B6;129-Ptprd $^{<\ tm1Yiw\ >}$ mice and were genotyped as described previously (Uetani et al., 2000). The primers used are the following: Delta-WT-F: 5′-CCAGCAGAGGCACAGAAACTC-3′; Delta-WT-R: 5′-CTGGAATTGTCT CACTTCCCTC-3′; Delta-Mut: 5′-GACTGCCTTGGGAAAAGCGCCTCC-3′. The C57BL/6N-A < tm1Brd > Ptprd < tm2a(KOMP)Wtsi > /WtsiOrl mice was purchased from Wellcome Trust Sanger Institute. The primers used are the following: Ptprd_111547_F: 5′- TCACCTCGCTGTTCTTCCTG-3′; Ptprd_111547_R: 5′- CTTCTCAGTGCCCAACCCTC-3′; CAS_R1_Term: 5′- TCGTGGTATCGT TATGCGCC-3′. For *in vitro* transfection, CD1 E12.5 pregnant mice respectively were obtained from Charles River Laboratory. All mice had free access to rodent chow and water in a 12 hour dark-light cycle room.

### Cortical precursor cell cultures

Cortical precursor cells were cultured as described previously (Barnabé-Heider and Miller, 2003; Cancino et al., 2015). Briefly, cortical precursor cells from cortices were dissected from embryonic day 12.5 CD1 or *Ptprd* mouse embryos in ice-cold HBSS and transfer into cortical precursor medium. The cortical precursor medium consisted of Neurobasal medium with 500 μM L-glutamine, 2% B27 supplement, 1% penicillin-streptomycin and 40 ng/ml FGF2. The dissected tissue was mechanically triturated by a

fire-polished glass pipette and plated onto 24-well plates coated with 2% laminin and 1% poly-D-lysine. Plating density of the cortical precursors was 150,000 cells/well for 24-well plates for single embryo cultures and plasmid transfections.

### Neurosphere cultures

E13.5 cortices from *Ptprd*$^{+/+}$, *Ptprd*$^{+/-}$ or *Ptprd*$^{-/-}$ embryos were dissected and mechanically dissociated into a single cell suspension by fire-polished glass pipette as previously described (Cancino et al., 2013, 2015). Cell density and viability were determined using trypan blue exclusion. Cells were seeded in triplicate at clonal density (10 cells/μl) in 6 well (2ml/well) ultra-low attachment culture plates (Coster) in serum-free medium supplemented with 20 ng/ml EFG, 10 ng/ml FGF2, 2% B27 supplement and 2 μg/ml heparin. Neurospheres were cultured for 6 days at 37°C. To evaluate self-renewal potential neurospheres were mechanically dissociated into single cell suspensions by fire-polished glass pipette, passed through a 45 μm nylon screen cell strainer, and cultured at clonal density of 2 cells/μl for additional 6 days.

## METHOD DETAILS

### Plasmid generation

The target sequence for murine *Ptprd* shRNA was cloned into pSUPER.retro.Neo+GFP. cDNAs encoding murine (pCMV-m PTPRD -Myc/DDK) and human PTPRD (pCMV-hPTPRD-Myc/DDK) were purchased from Origene. Murine PTPRD catalytic deficient mutant (pCMV-m PTPRD -ΔCD) was generated by deletion of the catalytic domain in murine PTPRD cDNA clone by restriction digestion and ligation. A cDNA encoding the catalytic domain of murine Ptprd (amino acids 1 to 522) was cloned from murine cDNA clone into pENTR-GST6P-1 (a gift from Eric Campeau) in frame, and later cloned into pEF-DEST51 by Gateway recombination cloning. Substrate trap mutants of PTPRD including D166A, C198S were constructed by standard site-directed mutagenesis PCR as described elsewhere. shMEK1/2 v2 neo was a gift from Kevin Janes. The target sequence for murine *TrkB* shRNA was cloned into into pLKO-UBI-GFP digested with EcoRI and PacI. pLKO-UBI-GFP was generated by digesting out hPGK promoter from pLKO.3G and ligating ubiquitin promoter (UBI) from pCLX-UBI-VenusN with PacI and BamHI. pLKO.3G was a gift from Christophe Benoist & Diane Mathis and and pCLX-UBI-VenusN was a gift from Patrick Salmon.

### Cortical precursor cell cultures transfection and quantification

For plasmid transfection of mouse cortical precursors, Lipofectamine LTX and Plus Reagent were used as described by the manufacturer. Briefly, 1 μg of DNA (1:2 ratio of EGFP to shRNA; 1:2 ration of EGFP to mouse *Ptprd* plasmids; 1:2:2 ration of EGFP, *Ptprd* shRNA and human *Ptprd* plasmids for rescue experiments; 1:2:2 ratio of EGFP, *Ptprd* shRNA and mouse PTPRD -ΔCD) and 1 μl of Lipofectamine LTX and Plus Regent in 100 μl of Opti-MEM were mixed, incubated for 20 min, and added to precursors three hours after plating. The target sequence for murine *Ptprd* shRNA was 5′- GGTTGAAAGCAAATGATAA-3′. The target sequence for the control shRNA was 5′-TCCCAACTGTCACGTTCTC-3′. The target sequence for murine *TrkB* was 5′-GCTCCTTAAGGATAACGAA-3′. The target sequence for murine *Mek1/2* shRNA was 5′-GCTGATCCACCTGGAGATCAA-3′. For quantification, immunostaining and image acquisition were performed, and > 100 cells per condition per experiment were counted and analyzed, and experiments were performed with 3 embryos per plasmid transfected and analyzed individually. For inhibition of MEK/ERK, PD98059 at 50 μm and Trametinib at 100 nM were added to precursors 4 hr after plating or transfections, and cultures were analyzed 3 days later. For quantification, immunostaining and image acquisition were performed, and > 100 cells per condition per experiment were counted and analyzed, and experiments were performed with 3 embryos per genotype or per plasmid transfected, and analyzed individually.

### *In Utero* Electroporation

In utero electroporation was performed as described previously (Gauthier et al., 2007; Yang et al., 2016). CD1 E13/14 mice were injected with a 1:3 ratio of nuclear EGFP plasmid with the shRNA and 0.5% trypan blue as a tracer. The square electroporator CUY EDIT (TR Teach, Japan) was used to deliver five 50 ms pluses of 40 V with 950 ms intervals per embryo. 3-4 days post electroporation, brains were dissected in ice-cold HBSS, fixed in 4% PFA at 4°C overnight, cryoprotected and cryosectioned coronally at 16-20 μm for histological analyses.

### Immunocytochemistry and histological analysis

For morphometric analysis, immunostaining of tissue sections was performed as described (Cancino et al., 2015; Gallagher et al., 2015; Yang et al., 2016). Briefly, brain sections were washed with TBS buffer, permeabilized with TBS, 0.3% Triton X-100 solution, and then incubated in TBS, 5% BSA, 0.3% Triton X-100 for 1 hour as a blocking solution. Brain slices were incubated with primary antibodies in blocking solution at 4°C overnight. After TBS washes, the sections were incubated with secondary antibodies in blocking solution for 1 hour at room temperature. Finally, after TBS washes, sections were mounted in Permount solution. In most cases, sections were counterstained with Hoechst 33258. Digital image acquisition was performed with Zen software (Carl Zeiss) on a Zeiss Axio Imager M2 microscope with a Hamamatsu Orca-Flash 4.0 CCD video camera or with Las X software (Leica microsystems) on a Leica DMi8 microscope. For BrdU treatment and quantification, pregnant dams from *Ptprd*$^{+/-}$ intercrosses were intraperitoneally injected with BrdU dissolved in PBS at the dose of 100 mg/kg of body weight at gestational day 13.5. The cortices of their embryos o litters were dissected at E13.5, E14.5, E15.5, E18.5 or P7 and processed for immunodetection of BrdU and other cell specific

markers. For quantification of precursor and neuron numbers, we analyzed sections at the medial-lateral level, counting all marker-positive cells in a 200 μm wide strip of the cortex extending from the meninges to the ventricle. In all cases, we analyzed at least 3 similar cortical sections/embryo or pup from 3 different embryos or pup per genotype (for a total of at least 9 sections per genotype). For Satb2 and Tbr1 immunostaining in P7 mice, the protocol was performed as mentioned before, and the image acquisition was performed with Las X software (Leica microsystems) on a Leica DMi8 microscope. For quantification of Satb2 and Tbr1-positive cells, we analyzed 2 similar sections of the somatosensory cortex per mice (Figure S3), using 3 different mice per genotype, and the cell number was quantified with CellProfiler software.

### Antibodies concentrations

The primary antibodies used for immunostaining were chicken anti-GFP (1:1000), rat anti-BrdU (1:200), rabbit anti- PTPRD (1:100), rabbit anti-Pax6 (1:1000), rabbit anti-Tbr2 (1:250), mouse anti-Ki67 (1:200), rabbit anti-Tbr1 (1:500), mouse anti-Satb2 (1:400), mouse anti-βIII-tubulin (1:1000), rabbit anti-βIII-tubulin (1:1000), rabbit anti-cleaved caspase 3 (1:200), rabbit anti-Sox2 (1:200), and goat anti-Sox2 (1:500). The secondary antibodies used for immunostaining were Alexa Fluor 555-conjugated donkey anti-mouse and anti-rabbit IgG (1:1000), Alexa Fluor 488-conjugated donkey anti-mouse, and anti-rabbit IgG (1:1000), Alexa Fluor 488-conjugated chicken anti-rat IgG (1:1000), and Cy3-conjugated donkey anti-goat antibody (1:1000). The primary antibodies used for immunoblotting were chicken anti-GFP (1:1000), rabbit anti-Ptprd (1:1000), rabbit anti Erk1/2 (1:5000), rabbit anti-TrkB (1:1000), rabbit anti-phospho-TrkB (1:1000), rabbit anti-PDGFR (1:1000), rabbit anti-phospho-PDGFR (1:1000), rabbit anti-MEK (1:1000), rabbit anti-phospho-MEK (1:1000), rabbit anti-phospho-ERK1/2 (1:000). The secondary antibodies used for immunoblotting were HRP-conjugated donkey anti-mouse and anti-rabbit IgG (1:1000).

### RT-PCR

Total RNA was isolated with Trizol and cDNA was prepared using the SuperScript III Reverse Transcriptase kit according to the manufacture's protocols. Primer sequences are following: PTPRD -F: 5′- CTTCAGTGCTGCTGTCTTGG-3′; PTPRD -R: 5′- TCATTTG CAGGAACATCAGG-3′; β-actin-F: 5′-GATGACGATATCGCTGCGCTG-3′; β-actin-R: 5′- GTACGACCAGAGGCATACAGG-3′. All PCR products were single bands with predicted molecular weights and confirmed by DNA sequencing.

### qRT-PCR

Total RNA was extracted with Tri-Reagent, treated with DNase I and cDNA was synthesized from 1 μg of RNA using the SuperScript IV Reverse Transcriptase Kit according to the manufacture's protocols. Quantitative PCR was performed using Taqman Fast Advance Mater Mix and Taqman probes targeted against either Ptprd (Mm01257868_m1) or β-Actin (Mm00607939_s1). β-Actin mRNA was used as an endogenous control for all reactions, and all reactions were performed in triplicate. Quantitative PCR was performed and analyzed using StepOne Plus Real-Time PCR system (Applied Biosystem).

### Western Blotting

Embryonic cortices or neurosphere cultures were lysated in RIPA buffer (50 mM Tris pH8, 150mM NaCl, 1% NP-40, 0.1% SDS, 1mM EDTA) containing 1mM PMSF (phenylmethanesulfonyl fluoride), 1mM sodium vanadate, 20mM sodium fluoride, 10 μg/ml aprotinin and 10 μg/ml leupeptin. 10-20 μg of protein lysate was electrophoresed, and western blots were performed as described previously (Barnabé-Heider and Miller, 2003).

### Substrate trapping

Substrate trapping mutants pEF-GST- PTPRD WT, pEF-GST- PTPRD D166A, pEF- PTPRD C198S were transfected and expressed in HEK293T cells. After transfection GST- PTPRD WT, GST- PTPRD D166A, GST- PTPRD C198S were extracted and purified with glutathione Sepharose 4b beads as suggested by the manufacturer. To trap PTPRD substrates, 200 μg of murine cortical lysate was incubated with 2 mg of purified GST- PTPRD WT, GST- PTPRD D166A, or GST- PTPRD C198S at 4°C overnight. After incubation the protein mixtures were incubated at 4°C for 2 h with glutathione Sepharose beads and purified as directed by the manufacturer.

## QUANTIFICATION AND STATISTICAL ANALYSIS

Statistics were performed using two-tailed Student's t test unless otherwise indicated in the text. To analyze the multi-group neuroanatomical studies, we used one-way ANOVA unless otherwise indicated in the text. Significant interactions or main effects were further analyzed using Newman-Keuls post hoc tests. All tests were performed using Prism 6 software. In all cases, error bars indicate standard error of the mean.

## DATA AND CODE AVAILABILITY

This study did not generate datasets.